

Unveiling the nature of *INTEGRAL* objects through optical spectroscopy*

IX. 22 more identifications, and a glance into the far hard X-ray Universe

N. Masetti¹, P. Parisi^{1,2,3}, E. Jiménez-Bailón⁴, E. Palazzi¹, V. Chavushyan⁵, L. Bassani¹, A. Bazzano³, A.J. Bird⁶, A.J. Dean⁶, G. Galaz⁷, R. Landi¹, A. Malizia¹, D. Minniti^{7,8,9}, L. Morelli^{10,11}, F. Schiavone¹, J.B. Stephen¹ and P. Ubertini³

¹ INAF – Istituto di Astrofisica Spaziale e Fisica Cosmica di Bologna, Via Gobetti 101, I-40129 Bologna, Italy

² Dipartimento di Astronomia, Università di Bologna, Via Ranzani 1, I-40127 Bologna, Italy

³ INAF – Istituto di Astrofisica Spaziale e Fisica Cosmica di Roma, Via Fosso del Cavaliere 100, I-00133 Rome, Italy

⁴ Instituto de Astronomía, Universidad Nacional Autónoma de México, Apartado Postal 70-264, 04510 México D.F., México

⁵ Instituto Nacional de Astrofísica, Óptica y Electrónica, Apartado Postal 51-216, 72000 Puebla, México

⁶ Physics & Astronomy, University of Southampton, Southampton, Hampshire, SO17 1BJ, United Kingdom

⁷ Departamento de Astronomía y Astrofísica, Pontificia Universidad Católica de Chile, Casilla 306, Santiago 22, Chile

⁸ Specola Vaticana, V-00120 Città del Vaticano

⁹ Department of Astrophysical Sciences, University of Princeton, Princeton, NJ 08544-1001, USA

¹⁰ Dipartimento di Astronomia, Università di Padova, Vicolo dell'Osservatorio 3, I-35122 Padua, Italy

¹¹ INAF-Osservatorio Astronomico di Padova, Vicolo dell'Osservatorio 5, I-35122 Padua, Italy

Received 1 December 2011; accepted 29 December 2011

ABSTRACT

Since its launch in October 2002, the *INTEGRAL* satellite has revolutionized our knowledge of the hard X-ray sky thanks to its unprecedented imaging capabilities and source detection positional accuracy above 20 keV. Nevertheless, many of the newly-detected sources in the *INTEGRAL* sky surveys are of unknown nature. The combined use of available information at longer wavelengths (mainly soft X-rays and radio) and of optical spectroscopy on the putative counterparts of these new hard X-ray objects allows us to pinpoint their exact nature. Continuing our long-standing program that has been running since 2004, and using 6 different telescopes of various sizes together with data from an online spectroscopic survey, here we report the classification through optical spectroscopy of 22 more unidentified or poorly studied high-energy sources detected with the IBIS instrument onboard *INTEGRAL*. We found that 16 of them are active galactic nuclei (AGNs), while the remaining 6 objects are within our Galaxy. Among the identified extragalactic sources, the large majority (14) is made up of Type 1 AGNs (i.e. with broad emission lines); of these, 6 lie at redshift larger than 0.5 and one (IGR J12319–0749) has $z = 3.12$, which makes it the second farthest object detected in the *INTEGRAL* surveys up to now. The remaining AGNs are of type 2 (that is, with narrow emission lines only), and one of the two cases is confirmed as a pair of interacting Seyfert 2 galaxies. The Galactic objects are identified as two cataclysmic variables, one high-mass X-ray binary, one symbiotic binary and two chromospherically active stars, possibly of RS CVn type. The main physical parameters of these hard X-ray sources were also determined using the multiwavelength information available in the literature. We thus still find that AGNs are the most abundant population among hard X-ray objects identified through optical spectroscopy. Moreover, we note that the higher sensitivity of the more recent *INTEGRAL* surveys is now enabling the detection of high-redshift AGNs, thus allowing the exploration of the most distant hard X-ray emitting sources and possibly of the most extreme blazars.

Key words. Galaxies: Seyfert — quasars: emission lines — X-rays: binaries — Stars: novae, cataclysmic variables — Stars: flare — X-rays: individuals

1. Introduction

One of the main objectives of the *INTEGRAL* mission (Winkler et al. 2003) is a regular survey of the whole sky in the hard X-ray band. This makes use of the unique imaging capability of the IBIS instrument (Ubertini et al. 2003) which allows the detection of sources at the mCrab¹ level with a typical localization accuracy of a few arcmin. The

Send offprint requests to: N. Masetti (masetti@iasfbo.inaf.it)

* Based on observations collected at the following observatories: Cerro Tololo Interamerican Observatory (Chile); Observatorio del Roque de los Muchachos of the Instituto de Astrofísica de Canarias (Canary Islands, Spain); Astronomical Observatory of Bologna in Loiano (Italy); Astronomical Observatory of Asiago (Italy); Observatorio Astronómico Nacional (San Pedro Mártir, México); Anglo-Australian Observatory (Siding Spring, Australia).

¹ 1 mCrab $\cong 2 \times 10^{-11}$ erg cm⁻² s⁻¹, with a slight dependence on the reference energy range.

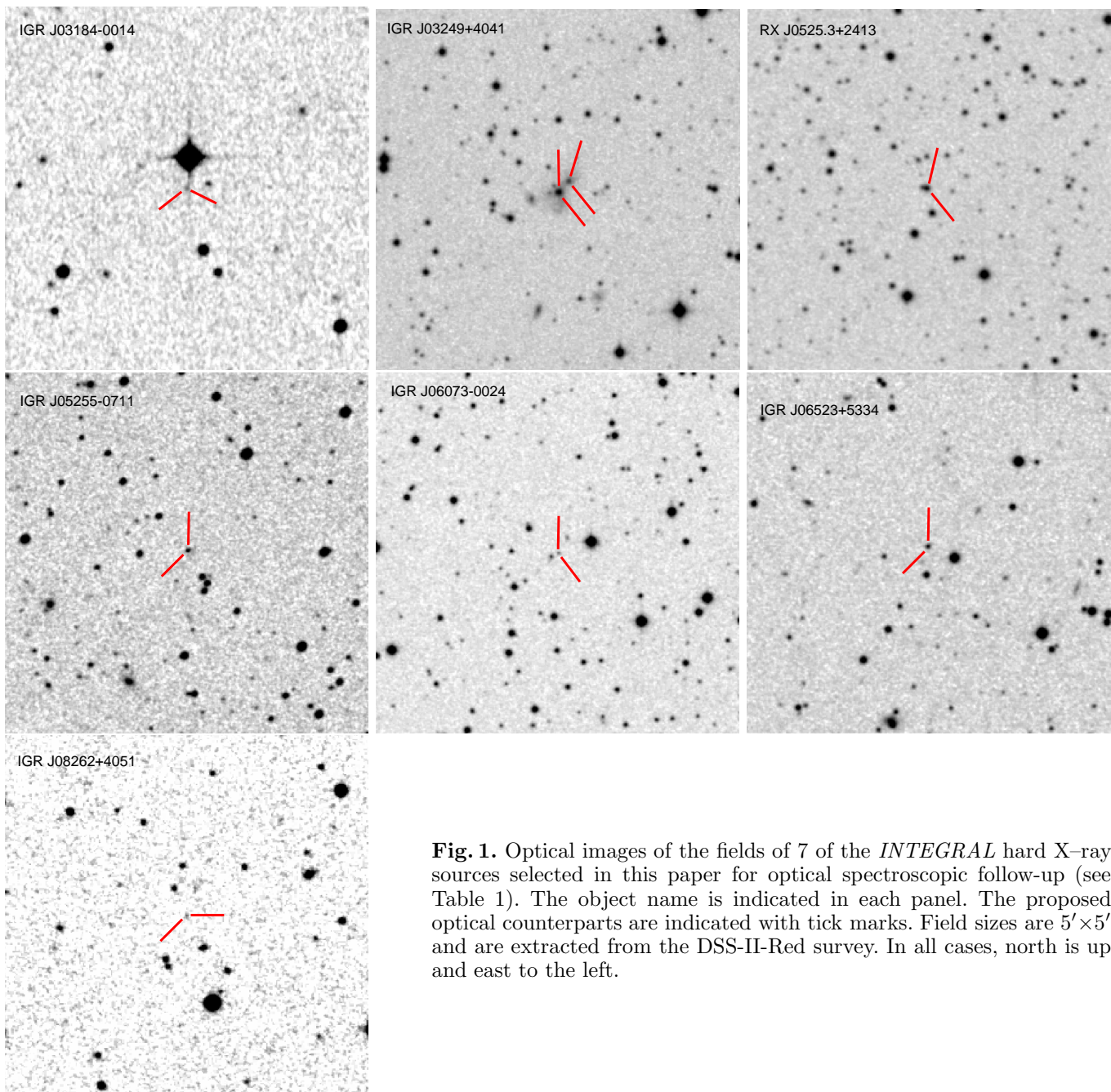


Fig. 1. Optical images of the fields of 7 of the *INTEGRAL* hard X-ray sources selected in this paper for optical spectroscopic follow-up (see Table 1). The object name is indicated in each panel. The proposed optical counterparts are indicated with tick marks. Field sizes are $5' \times 5'$ and are extracted from the DSS-II-Red survey. In all cases, north is up and east to the left.

latest (4th of the series) IBIS catalogue published up to now by Bird et al. (2010) contains more than 700 hard X-ray sources detected in the 20–100 keV band down to an average flux level of about 1 mCrab and with positional accuracy better than ~ 5 arcmin.

However, a substantial fraction ($\sim 30\%$) of them had no obvious counterpart at other wavelengths and therefore could not yet be associated with any known class of high-energy emitting objects. A similar situation is present in the 7-year *INTEGRAL*/IBIS all-sky survey of Krivonos et al. (2010)², obtained with a parallel (and partially overlapping) *INTEGRAL* data set and which contains more than 500 sources (in part coincident with those in Bird et al. 2010).

² An up-to-date online version of this catalog can be found at <http://hea.iki.rssi.ru/integral/survey/catalog.php>

Therefore, a multiwavelength observational campaign on these unidentified sources is fundamental to pinpoint their nature, and is especially important given that they build up to one third of the whole set of IBIS detections.

X-ray analysis methods have shown their usefulness in identifying the nature of new *INTEGRAL* sources, such as for example X-ray timing by the detection of pulsations, orbital periods or X-ray bursts (e.g., Walter et al. 2006; Sguera et al. 2007; Del Santo et al. 2007; Chenevez et al. 2007; Bird et al. 2009; La Parola et al. 2010), or X-ray spectroscopy and imaging (see for instance Tomsick et al. 2009, Rodriguez et al. 2010a, Malizia et al. 2010, Fiocchi et al. 2010, and references therein). Alternatively, and also quite effectively, cross-correlation with soft X-ray catalogs and consequently optical spectroscopy on thereby selected candidates allows the determination of the nature

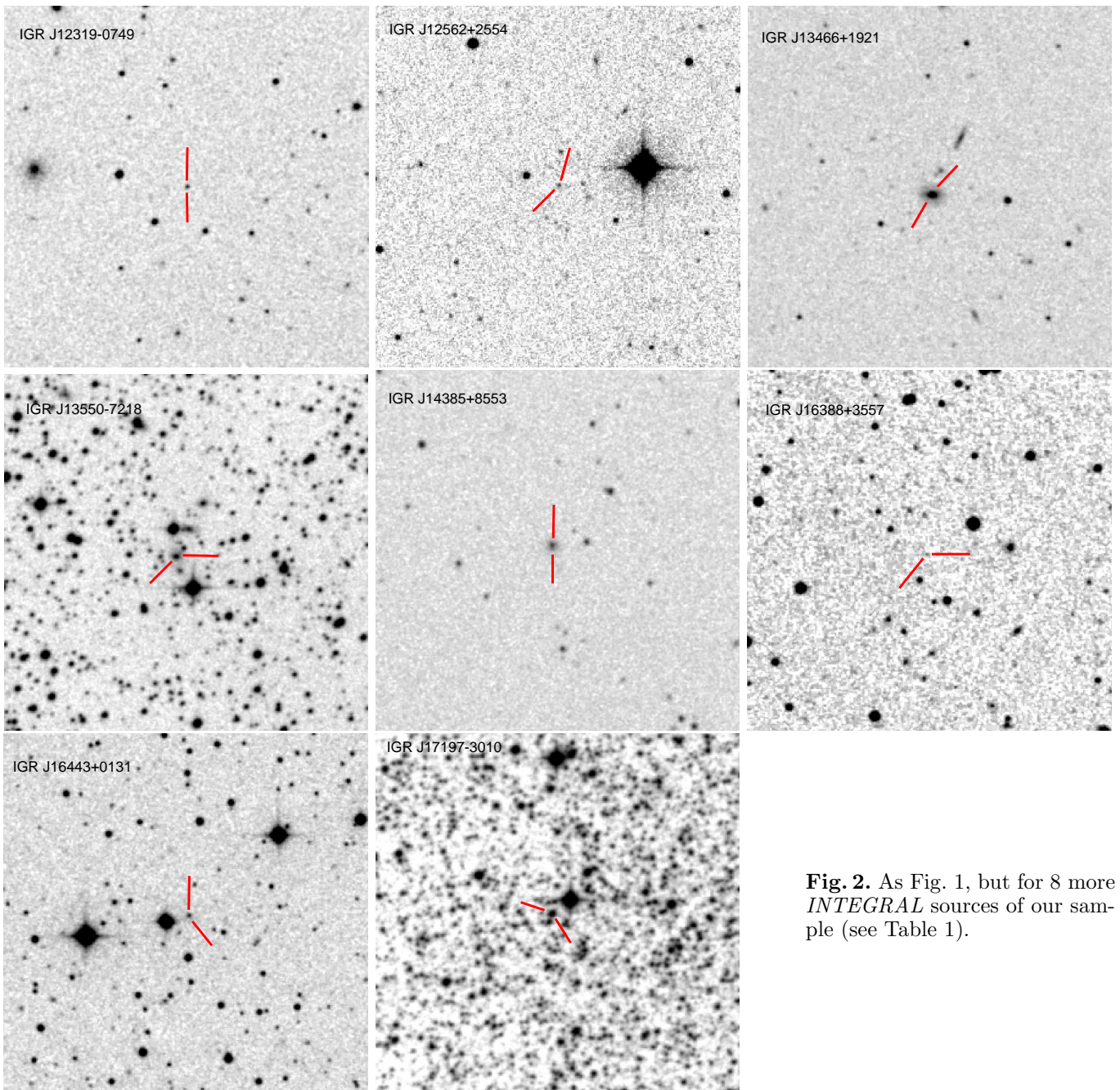


Fig. 2. As Fig. 1, but for 8 more *INTEGRAL* sources of our sample (see Table 1).

and the main multiwavelength characteristics of unidentified or poorly studied hard X-ray objects.

Here, we continue the identification work on *INTEGRAL* sources we started in 2004 and which permitted us to, so far, identify more than 150 sources by means of optical spectroscopy (see Masetti et al. 2004, 2006abcd, 2008a, 2009, 2010 [hereafter Papers I-VIII, respectively]; Masetti et al. 2007, 2008b; Maiorano et al. 2011). We report here on optical spectra of firm or likely counterparts of 22 unidentified, unclassified or poorly studied sources belonging to one or more IBIS surveys (Bird et al. 2007, 2010; Krivonos et al. 2010); we also added to our sample the unidentified source IGR J19173+0747 reported in Pavan et al. (2011). Optical spectroscopy for these objects was acquired using 6 different telescopes and one public spectroscopic archive.

The paper is structured as follows. In Sect. 2 we explain the criteria used to choose the sample of *INTEGRAL* and optical objects considered in this work. In Sect. 3 a brief description of the observations is presented. Section 4 illustrates and discusses the results together with an update of the statistical outline of the identifications of *INTEGRAL* sources obtained until now. Conclusions are reported in Sect. 5.

As in our previous Papers I-VIII on the subject, the main results of this work, along with the information about the *INTEGRAL* sources that have been identified (by us or by other groups) using optical or near-infrared (NIR) observations, are listed in a web page³ that we maintain as a service to the scientific community (Masetti & Schiavone 2008).

³ <http://www.iasfbo.inaf.it/extras/IGR/main.html>

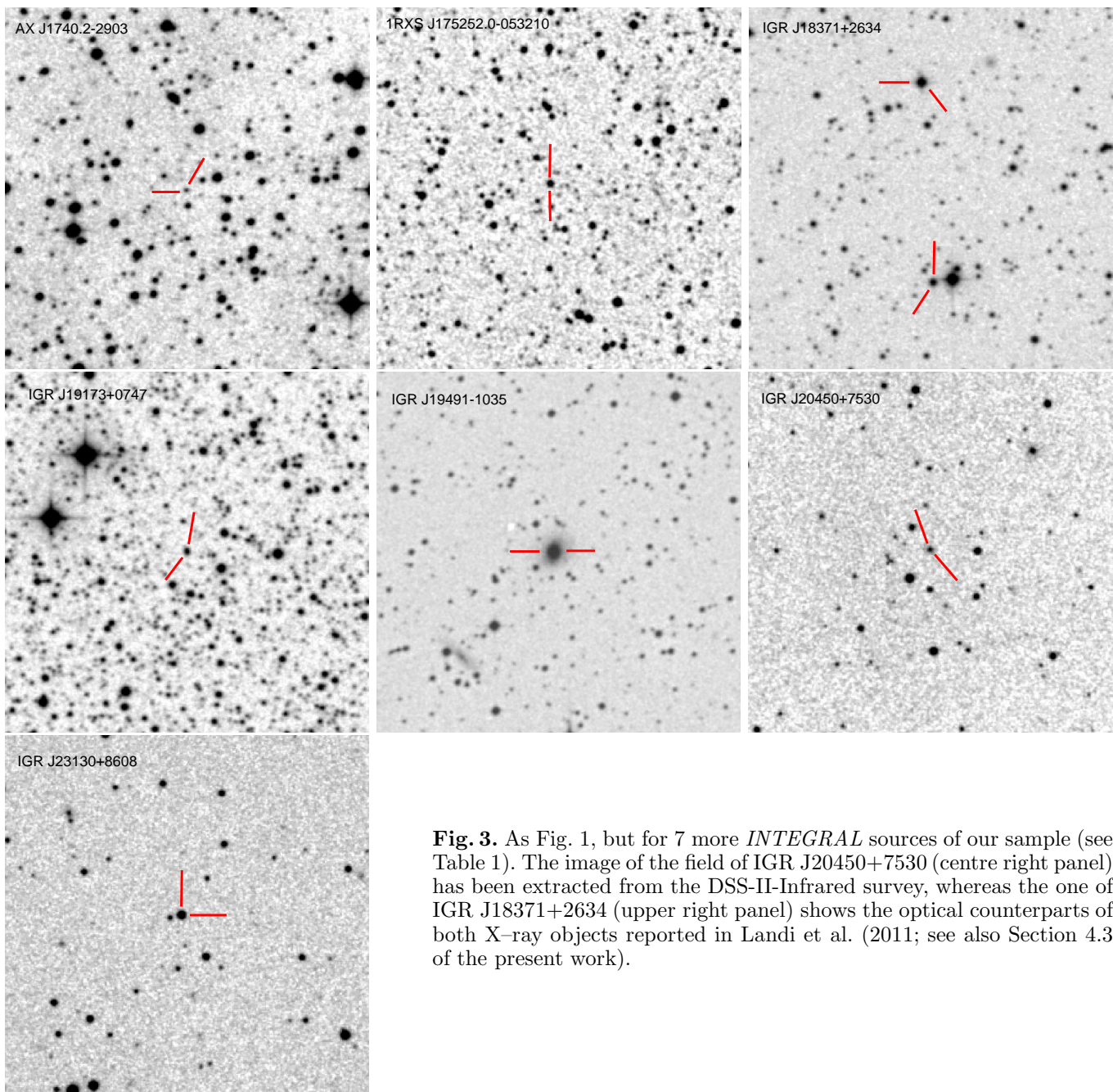


Fig. 3. As Fig. 1, but for 7 more *INTEGRAL* sources of our sample (see Table 1). The image of the field of IGR J20450+7530 (centre right panel) has been extracted from the DSS-II-Infrared survey, whereas the one of IGR J18371+2634 (upper right panel) shows the optical counterparts of both X-ray objects reported in Landi et al. (2011; see also Section 4.3 of the present work).

In this paper, unless otherwise stated, errors and limits are reported at 1σ and 3σ confidence levels, respectively. We also note that this work supersedes the results presented in the preliminary analyses of Parisi et al. (2010) and Masetti et al. (2011).

2. Sample selection

Using the same approach we applied in our previous Papers I-VIII, we considered the IBIS surveys of Bird et al. (2007, 2010) and Krivonos et al. (2010), and we selected unidentified or unclassified hard X-ray sources that contain, within the IBIS 90% confidence level error box, a single bright soft X-ray object detected either in the *ROSAT* all-sky surveys (Voges et al. 1999, 2000), or with *Swift*/XRT (from Page et al. 2007, Lutovinov et al. 2010, Rodriguez et al. 2010ab, Landi et al. 2010abc, 2011, Krivonos et al. 2011, as well as

from the XRT archive⁴), or in the Slew Survey (Saxton et al. 2008) or Serendipitous Source Catalog (Watson et al. 2009) of *XMM-Newton*, or with pointed *Chandra* (Fiocchi et al. 2010) and *XMM-Newton* (Halpern & Gotthelf 2010; Farrell et al. 2010) observations. This approach was proven by Stephen et al. (2006) to be very effective in associating, with a high degree of probability, IBIS sources with a softer X-ray counterpart and in turn drastically reducing their positional error circles to better than a few arcsec in radius, making the search area smaller by a factor of $\sim 10^4$.

After this first selection, we chose among these objects those that had, within their refined 90% confidence level

⁴ XRT archival data are freely available at <http://www.asdc.asi.it/>

soft X-ray error boxes⁵, a single possible optical counterpart with magnitude $R \lesssim 20$ in the DSS-II-Red survey⁶, so that optical spectroscopy could be obtained with reasonable signal-to-noise ratio (S/N) with telescopes having aperture of at least 1.5 metres. This allowed us to select 13 IBIS sources.

We moreover added the newly-discovered source IGR J19173+0747 (Pavan et al. 2011) to our list, as these authors also report an arcsecond-sized position obtained with *Swift* and a possible optical counterpart.

To increase the size of this sample, we then used the following independent approaches.

First, we cross-correlated the above IBIS surveys with radio catalogs such as the NVSS (Condon et al. 1998), SUMSS (Mauch et al. 2003), and MGPS (Murphy et al. 2007) surveys when a soft X-ray observation of the hard X-ray source field was not available. This step provided 1 more *INTEGRAL* source (IGR J06073–0024) with a likely optical counterpart. In a few cases (e.g. IGR J13550–7218; Landi et al. 2010d), the use of this method on the IBIS sources already selected allowed us to further reduce the soft X-ray position uncertainty down to less than $2''$ and thus to pinpoint the actual counterpart with a higher degree of certainty.

Next, we relaxed the search described above by considering the IBIS 99% error circles. This allowed us to pinpoint 7 further cases to be followed up with optical spectroscopy (see also Rodriguez et al. 2010a, Flocchi et al. 2010, and Landi et al. 2010a, 2011).

We wish to point out that the 8 sources thus selected should be considered to have only a tentative, albeit likely, counterpart: this is indicated with an asterisk alongside their names in Table 1 and by a question mark near the name of the corresponding hard X-ray source in the optical spectra of Figs. 4, 5, 7 and 8. This caution should particularly be applied to the IBIS source selected using radio surveys (but see Maiorano et al. 2011), as no thorough statistical study on the confidence of the hard X-ray/radio positional correlation is available up to now for the IBIS catalogues. The reader is moreover referred to Paper III for the caveats and the shortcomings of choosing, within an IBIS error box, “peculiar” sources that are not straightforwardly linked to an arcsec-sized soft X-ray position.

Thus, in total we gathered a sample of 22 *INTEGRAL* objects with possible optical counterparts, which we explored by means of optical spectroscopy. Their names and accurate coordinates (to $0''.2$ or better; see next section) are reported in Table 1, while their optical finding charts are shown in Figs. 1-3, with the corresponding putative counterparts indicated with tick marks.

Finally, we stress here that in our final sample there are 5 *INTEGRAL* sources (IGR J03249+4041, Lutovinov et al. 2010; RX J0525.3+2413, Torres et al. 2007; IGR J06253+5334, Halpern 2011; AX J1740.2–2903, Halpern & Gotthelf 2010; and IGR J19491–1035, Krivonos et al. 2011) that, although already identified by these authors, have incomplete information at longer wavelengths or were

independently observed by us before their identification was published. Our observations are thus presented here to confirm the nature of these objects and to improve their classification and the amount of information known about them.

3. Optical spectroscopy

Analogously to Papers VI-VIII, almost all of the data presented in this work were collected in the course of a campaign that lasted more than one year (between March 2010 and August 2011) and that involved observations at the following telescopes:

- the 1.5m at the Cerro Tololo Interamerican Observatory (CTIO), Chile;
- the 1.52m “Cassini” telescope of the Astronomical Observatory of Bologna, in Loiano, Italy;
- the 1.82m “Copernicus” telescope of the Astronomical Observatory of Asiago, Italy;
- the 2.1m telescope of the Observatorio Astronómico Nacional in San Pedro Martir (SPM), México;
- the 3.58m “Telescopio Nazionale Galileo” (TNG) at the Roque de Los Muchachos Observatory in La Palma, Spain;
- the 10.4m “Gran Telescopio Canarias” (GTC), again at the Roque de Los Muchachos Observatory in La Palma, Spain;

The spectroscopic data acquired at these telescopes have been optimally extracted (Horne 1986) and reduced following standard procedures using IRAF⁷. Calibration frames (flat fields and bias) were taken on the day preceding or following the observing night. The wavelength calibration was performed using lamp data acquired soon after each on-target spectroscopic acquisition; the uncertainty in this calibration was $\sim 0.5 \text{ \AA}$ in all cases according to our checks made using the positions of background night sky lines. Flux calibration was performed using catalogued spectrophotometric standards.

The spectrum of the optical counterpart of IGR J19491–1035 was retrieved from the Six-degree Field Galaxy Survey⁸ (6dFGS) archive (Jones et al. 2004), collected using the 3.9m Anglo-Australian Telescope of the Anglo-Australian Observatory in Siding Spring (Australia). Since the 6dFGS archive provides spectra that are not flux-calibrated, we used the optical photometric information in Jones et al. (2005) to calibrate the spectrum of this object.

In Table 1, we provide a detailed log of all the observations. Column 1 indicates the names of the observed *INTEGRAL* sources. In Cols. 2 and 3 we list the possible optical counterpart coordinates, extracted from the 2MASS (with an accuracy of $\leq 0''.1$, according to Skrutskie et al. 2006) or USNO catalogs (with uncertainties of about $0''.2$: Deutsch 1999; Assafin et al. 2001; Monet et al. 2003). The telescope and instrument used for the observations are reported in Col. 4, while characteristics of each spectrograph are presented in Cols. 5 and 6. Column 7 reports the observation date and the UT time at mid-exposure, and Col. 8

⁵ When needed, for the cases in which the soft X-ray positional error is given at 1σ confidence level (basically, the *ROSAT* and *XMM-Newton* Slew Survey sources) we rescaled it to the corresponding 90% confidence level assuming a Gaussian probability distribution.

⁶ Available at <http://archive.eso.org/dss/dss>

⁷ IRAF is the Image Reduction and Analysis Facility made available to the astronomical community by the National Optical Astronomy Observatories, which are operated by AURA, Inc., under contract with the U.S. National Science Foundation. It is available at <http://iraf.noao.edu/>

⁸ <http://www.aao.gov.au/local/www/6df/>

Table 1. Log of the spectroscopic observations presented in this paper (see text for details).

(1) Object	(2) RA (J2000)	(3) Dec (J2000)	(4) Telescope+instrument	(5) λ range (Å)	(6) Disp. (Å/pix)	(7) UT Date & Time at mid-exposure	(8) Exposure time (s)
IGR J03184–0014*	03:18:17.54	–00:17:50.2	GTC+OSIRIS	3600-10000	5.2	05 Sep 2010, 06:25	3×300
IGR J03249+4041: LEDA 4678815	03:25:12.23	+40:42:02.2	SPM 2.1m+B&C Spec.	3500-7800	4.0	01 Nov 2010, 11:33	2×1800
LEDA 97012	03:25:12.96	+40:41:52.8	SPM 2.1m+B&C Spec.	3500-7800	4.0	01 Nov 2010, 10:28	2×1800
IGR J05255–0711*	05:25:09.77 [†]	–07:07:45.1 [†]	TNG+DOLoReS	3800-8000	2.5	09 Oct 2010, 03:27	3×1200
RX J0525.3+2413	05:25:22.70	+24:13:33.3	SPM 2.1m+B&C Spec.	3500-7800	4.0	31 Oct 2010, 10:24	2×1800
IGR J06073–0024*	06:06:57.43 [†]	–00:24:57.7 [†]	TNG+DOLoReS	3800-8000	2.5	01 Dec 2010, 00:19	3×1500
IGR J06523+5334	06:52:31.40	+53:31:31.5	SPM 2.1m+B&C Spec.	3500-7800	4.0	13 Mar 2010, 04:18	3×1800
IGR J08262+4051	08:26:17.92 [†]	+40:47:58.8 [†]	TNG+DOLoReS	3800-8000	2.5	01 Dec 2010, 02:07	3×1800
IGR J12319–0749	12:31:57.71 [†]	–07:47:18.0 [†]	TNG+DOLoReS	3800-8000	2.5	01 Jan 2011, 05:14	840
IGR J12562+2554*	12:56:10.43 [†]	+26:01:03.7 [†]	GTC+OSIRIS	3600-10000	5.2	26 Dec 2010, 05:07	2×300
IGR J13466+1921	13:46:28.43	+19:22:43.1	SPM 2.1m+B&C Spec.	3500-7800	4.0	13 Mar 2010, 10:33	2×1800
IGR J13550–7218	13:55:13.53	–72:19:15.0	CTIO 1.5m+RC Spec.	3300-10500	5.7	09 Feb 2011, 07:23	2×1500
IGR J14385+8553*	14:44:27.71	+86:00:56.5	Copernicus+AFOSC	3500-7800	4.2	01 Mar 2011, 23:41	2×1200
IGR J16388+3557*	16:38:21.23 [†]	+36:02:26.4 [†]	TNG+DOLoReS	3800-8000	2.5	1 Aug 2011, 00:09	2×1800
IGR J16443+0131	16:44:37.93	+01:29:01.4	TNG+DOLoReS	3800-8000	2.5	11 Jun 2011, 04:24	2×1200
IGR J17197–3010*	17:19:51.83	–30:02:00.3	SPM 2.1m+B&C Spec.	3500-7800	4.0	16 Jul 2010, 04:37	2×1800
AX J1740.2–2903	17:40:16.11 [†]	–29:03:37.9 [†]	SPM 2.1m+B&C Spec.	3500-7800	4.0	17 Jul 2010, 06:05	2400
1RXS J175252.0–053210	17:52:52.47	–05:32:06.4	SPM 2.1m+B&C Spec.	3500-7800	4.0	15 Mar 2010, 11:57	2×1800
IGR J18371+2634*	18:37:28.88	+26:32:29.0	Cassini+BFOSC	3500-8700	4.0	07 May 2011, 23:52	2×1200
IGR J19173+0747	19:17:20.78	+07:47:50.7	SPM 2.1m+B&C Spec.	3500-7800	4.0	14 Jul 2010, 08:22	2×1800
IGR J19491–1035	19:49:09.27	–10:34:25.0	AAT+6dF	3900-7600	1.6	15 Jun 2004, 12:10	1200+600
IGR J20450+7530	20:44:34.41	+75:31:58.9	Cassini+BFOSC	3500-8700	4.0	03 Aug 2010, 00:09	1800
IGR J23130+8608	23:08:59.80	+86:05:52.6	TNG+DOLoReS	3800-8000	2.5	01 Sep 2010, 23:05	3×1500

Note: if not indicated otherwise, source coordinates were extracted from the 2MASS catalog and have an accuracy better than $0''.1$.

*: tentative association (see text).

[†]: coordinates extracted from the USNO catalogs, having an accuracy of about $0''.2$ (Deutsch 1999; Assafin et al. 2001; Monet et al. 2003).

provides the exposure times and the number of observations for each source.

For the source naming in Table 1, we adopted the names as they are reported in the relevant surveys (Bird et al. 2007, 2010; Krivonos et al. 2010) or papers (Pavan et al. 2011), and the “IGR” alias when available.

4. Results

In the following, we give a description of the adopted identification and classification criteria for the optical spectra of the selected sources. They are basically the same as in our previous papers (I–VIII); however, for the sake of clarity we briefly list them again. The optical magnitudes quoted below, if not stated otherwise, are extracted from the USNO-A2.0 catalog⁹.

To evaluate the reddening along the line of sight for the Galactic sources in our sample, when possible and applicable, we considered an intrinsic H_α/H_β line ratio of 2.86 (Osterbrock 1989) and inferred the corresponding color excess by comparing the intrinsic line ratio with the measured one by applying the Galactic extinction law of Cardelli et al. (1989).

To determine the distances of the compact Galactic X-ray sources of our sample, for Cataclysmic Variables (CVs) we assumed an absolute magnitude $M_V \sim +9$ and an intrinsic color index $(V - R)_0 \sim 0$ mag (Warner 1995), whereas for the single high-mass X-ray binary (HMXB) and symbiotic star of our sample we used the intrinsic stellar color indices and absolute magnitudes reported in Lang (1992), Wegner (1994) and Ducati et al. (2001). For the ac-

tive stars identified in our selection of sources we assumed similarity with object II Peg, as suggested in Rodriguez et al. (2010a). Although these methods basically provide an order-of-magnitude value for the distance of Galactic sources, our past experience (Papers I–VIII) tells us that these estimates are in general correct to within 50% of the refined value subsequently determined with more precise approaches.

For the classification of active galactic nuclei (AGNs), we used the criteria of Veilleux & Osterbrock (1987) and the line ratio diagnostics of both Ho et al. (1993, 1997) and Kauffmann et al. (2003) and, for assigning the subclasses of Seyfert 1 galaxies, we used the $H_\beta/[O\ III]\lambda 5007$ line flux ratio criterion described in Winkler (1992).

The AGN spectra shown here were not corrected for starlight contamination (see, e.g., Ho et al. 1993, 1997) because of the limited S/N and spectral resolution. We do not expect this to affect any of our main results and conclusions.

In the following, we consider a cosmology with $H_0 = 65$ km s^{–1} Mpc^{–1}, $\Omega_\Lambda = 0.7$, and $\Omega_m = 0.3$; the luminosity distances of the extragalactic objects reported in this paper were computed for these parameters using the Cosmology Calculator of Wright (2006). When not explicitly stated otherwise, for our X-ray flux estimates we assume a Crab-like spectrum except for the *XMM-Newton* sources, for which we considered the fluxes reported in Saxton et al. (2008) or in Watson et al. (2009). The X-ray luminosities reported in Tables 2, 3, 4, 6, 7 and 8 are associated with a letter indicating the satellite and/or the instrument with which the measurement of the corresponding X-ray flux was obtained, namely *ASCA* (A), *Swift*/BAT (B), *Chandra* (C), *INTEGRAL* (I), *XMM-Newton* (N), *ROSAT* (R), and *Swift*/XRT (X).

⁹ available at:
<http://archive.eso.org/skycat/servers/usnoa>

Hereafter, we present the object identifications by dividing them into three broad classes (AGNs, accreting binaries, and other Galactic objects).

4.1. AGNs

We found that 16 objects in our sample have optical spectra that allow us to classify them as AGNs (see Figs. 4-6): indeed, all of them exhibit strong, redshifted broad and/or narrow emission lines typical of nuclear galactic activity: 14 of them can be classified as Type 1 (broad-line) and 2 as Type 2 (narrow-line) AGNs; in detail, see Table 2 for the breakdown of low-redshift Type 1 AGNs in terms of subclasses.

Moreover, we stress that 6 of the broad-line AGN identified here lie at high redshift ($z > 0.5$, and in four cases $z > 1$; see Table 3). In particular, our data allow us to state that IGR J12319–0749, at redshift $z = 3.12$, is the second most distant and persistently emitting hard X-ray object detected by *INTEGRAL* up to now, after the blazar IGR J22517+2218, which lies at redshift $z = 3.668$ (Bassani et al. 2007 and references therein).

The main observed and inferred parameters for each of these two broad classes of AGNs are reported in Tables 2-4. In these tables, X-ray luminosities were computed from the fluxes reported in Voges et al. (1999, 2000), *ROSAT* Team (2000), Bird et al. (2007, 2010), Saxton et al. (2008), Watson et al. (2009), Cusumano et al. (2010), Krivonos et al. (2010, 2011), Focchi et al. (2010), Landi et al. (2010abc, 2011), Rodriguez et al. (2010ab), and Tueller et al. (2010).

For the large majority of the AGNs in our sample (that is, 13 out of 16), the redshift value was determined in this work for the first time. The redshifts of the remaining 3 cases are consistent with those reported in the literature (Lutovinov et al. 2010; Halpern 2011; Krivonos et al. 2011). We also give here a more accurate classification of the sources IGR J06523+5334 and IGR J19491–1035, independently identified by Halpern (2011) and Krivonos et al. (2011), respectively: both are Seyfert 1.2 galaxies.

When we examined the optical and X-ray properties of the AGN sources of our sample in detail, we found the following noteworthy issues for some selected cases.

Concerning narrow emission line galaxies, we confirm the double Seyfert 2 nature of the interacting galaxy pair LEDA 97012 and LEDA 4678815, associated with the *INTEGRAL* source IGR J03249+4041, as first proposed by Lutovinov et al. (2010).

Moreover, we found that LEDA 3075535 (the counterpart of IGR J13550–7218) does not appear to show any substantial reddening local to the AGN (see Table 4). This suggests that this source may be a “naked” Seyfert 2 galaxy (e.g., Panessa & Bassani 2002, Bianchi et al. 2008), i.e. an AGN that lacks the broad-line region (BLR): these objects, despite first appearances, are not rare among the sources detected with *INTEGRAL* (see for instance Paper VI). It may be noted that Rodriguez et al. (2010b) found a relatively high column density ($N_{\text{H}} \sim 2 \times 10^{23} \text{ cm}^{-2}$) in the X-ray spectrum of IGR J13550–7218: this differs from our optical result, although an X-ray spectrum with higher S/N is mandatory for a definite comparison between the two estimates.

Using the diagnostic T of Bassani et al. (1999), that is, the ratio of the measured 2–10 keV X-ray flux to the unabsorbed flux of the [O III] λ 5007 forbidden emission line, we

can determine the Compton nature of the Seyfert 2 AGNs in our sample. After correcting the [O III] λ 5007 emission line flux of LEDA 97012, LEDA 4678815 and LEDA 3075535 for the absorption local to the corresponding AGN (see Table 4), we found that the parameter T has values 0.005, 7.0 and 9.6, respectively, indicating that LEDA 97012 is likely a Compton thick source, whereas the other two AGNs are in the Compton thin regime. We remark that the figures above should be considered as upper limits to the actual values of T because the X-ray fluxes that we used refer to bands which are wider than the ones for which this method is intended to be applied (see Table 4).

These results can be checked following an independent method, that is, the diagnostic of Malizia et al. (2007), which uses the ratio of the flux measurement in the 2–10 keV band to that in the 20–100 keV band. For this parameter we found values of 0.007, 0.33, and 0.14, respectively, for the three sources considered above: comparing these numbers with those of the sample of Malizia et al. (2007, their Fig. 5), we again found that the one corresponding to LEDA 97012 falls in the locus in which possible Compton thick AGNs are segregated. This result therefore independently confirms those obtained with the method of Bassani et al. (1999). Once again, we caution the reader that, despite the definition of the diagnostic of Malizia et al. (2007), the X-ray fluxes available allow us to actually compute strict upper limits to the above ratio. We also note that, for galaxies LEDA 97012 and LEDA 4678815, we used in the above computations their combined hard X-ray flux detected by *INTEGRAL* as IGR J03249+4041.

With regards to the galaxy LEDA 97012, it should be noted that Malizia et al. (in preparation) found an upper limit for its local hydrogen column density ($< 1.5 \times 10^{21} \text{ cm}^{-2}$) which argues against a Compton Thick interpretation for this AGN. However, the difference with our results can be (at least partially) explained by the relatively low S/N of the spectra, and by the source confusion produced by the vicinity to LEDA 4678815, the other X-ray emitting AGN in this galaxy pair. Thus, a clearer analysis on this issue may only be obtained using X-ray satellites affording very high angular resolution such as *Chandra*.

Regarding the broad-line AGNs of our sample, we point out that according to Landi et al. (2010a), of the soft X-ray sources which are found within the 99% error circle of IGR J05255–0711, only one (source #2; see also Table 1) has detectable emission above 3 keV, and this object is indeed the one for which we report the optical spectrum in Fig. 5, upper left panel. Actually, we also acquired spectroscopy for the source labeled #1 by Landi et al. (2010a) with the 1.5m CTIO telescope on 17 October 2010: the data show that it is a Galactic star with no peculiarities. Therefore we will not discuss this object further.

Finally, we applied the prescriptions of Wu et al. (2004) and Kaspri et al. (2000), which use the width and the strength of the broad component of the H_{β} emission as a probe of the orbital velocity and the size of the BLR (this procedure could not be applied to IGR J03184–0014 as no broad H_{β} emission component was detected in its spectrum). In the cases in which H_{β} falls outside the optical range covered by our spectroscopy, we apply the formulae of McLure & Jarvis (2002) or Vestergaard (2002) which use the information conveyed by the Mg II or C IV broad emissions, respectively. With these approaches we thus cal-

Table 2. Synoptic table containing the main results for the 8 low- z broad emission-line AGNs (Fig. 4) identified or observed in the present sample of *INTEGRAL* sources.

Object	$F_{H\alpha}$	$F_{H\beta}$	$F_{[OIII]}$	Class	z	D_L (Mpc)	$E(B - V)_{Gal}$	L_X
IGR J03184-0014	* *	<0.05 [<0.07]	0.11±0.02 [0.14±0.02]	Sy1.9	0.330	1867.2	0.063	6.3 (2-10; X) 1200 (20-40; I) <880 (40-100; I)
IGR J06523+5334	— —	10.0±1.0 [11.8±1.2]	3.6±0.3 [4.2±0.4]	Sy1.2	0.301	1678.6	0.062	5.4 (0.1-2.4; R) 5.7 (2-10; X) 740 (20-40; I) <870 (40-100; I)
IGR J13466+1921	* *	39±4 [42±4]	14.6±1.0 [15.5±1.1]	Sy1.2	0.085	417.1	0.024	0.73 (0.1-2.4; R) 33 (17-60; I) 23 (14-195; B)
IGR J14385+8553	* *	11.5±1.7 [20±3]	7.4±0.7 [12.4±1.2]	Sy1.5	0.081	396.4	0.191	6.9 (0.2-12; N) <10 (20-40; I) <21 (40-100; I)
IGR J16443+0131	— —	1.2±0.2 [1.8±0.3]	1.60±0.16 [1.9±0.2]	Sy1.5	0.342	1946.5	0.071	12 (2-10; X) 340 (20-40; I) <430 (40-100; I)
1RXS J175252.0-053210	* *	20±2 [370±40]	6.0±1.0 [100±20]	Sy1.2	0.136	690.2	0.995	2.7 (0.1-2.4; R) 57 (20-100; I)
IGR J19491-1035	* *	220±20 [480±50]	510±50 [1000±100]	Sy1.2	0.0240	112.7	0.238	1.2 (2-10; X) 1.7 (17-60; I)
IGR J20450+7530	* *	11±2 [35±8]	<3 [<10]	Sy1	0.095	469.3	0.382	0.84 (2-10; X) 53 (20-40; I) <42 (40-100; I)

Note: emission-line fluxes are reported both as observed and (between square brackets) corrected for the intervening Galactic absorption $E(B - V)_{Gal}$ along the object line of sight (from Schlegel et al. 1998). Line fluxes are in units of 10^{-15} erg cm^{-2} s^{-1} , whereas X-ray luminosities are in units of 10^{43} erg s^{-1} and the reference band (between round brackets) is expressed in keV.

In the last column, the upper-case letter indicates the satellite and/or the instrument with which the corresponding X-ray flux measurement was obtained (see text).

The typical error in the redshift measurement is ± 0.001 but for the 6dFGS spectrum, for which an uncertainty of ± 0.0003 can be assumed.

*: heavily blended with [N II] lines

Table 3. Synoptic table containing the main results for the 6 high-redshift broad-line QSOs ($z > 0.5$; Fig. 5) identified in the present sample of *INTEGRAL* sources.

Object	$F_{H\beta}$	F_{MgII}	F_{CIII}	F_{CIV}	z	D_L (Mpc)	$E(B - V)_{Gal}$	L_X
IGR J05255-0711	4.3±0.4 4.9±0.5	5.5±0.5 7.4±0.7	— —	— —	0.634	4065.0	0.113	32 (2-10; X) 4000 (20-40; I) <4700 (40-100; I)
IGR J06073-0024	— —	2.2±0.2 [7.2±0.7]	1.9±0.4 [12±3]	— —	1.028	7362.5	0.438	7800 (20-40; I) <14000 (40-100; I)
IGR J08262+4051	— —	1.65±0.17 [1.90±0.19]	2.4±0.2 [2.6±0.3]	—	1.038	7451.1	0.042	6600 (20-40; I) <11000 (40-100; I)
IGR J12319-0749	— —	— —	— —	0.9±0.3 [1.0±0.3]	3.12	28692.5	0.023	5300 (0.1-2.4; R) 44000 (20-40; I) <46000 (40-100; I)
IGR J12562+2554	— —	6.1±0.3 [6.3±0.3]	3.0±0.4 [3.2±0.4]	—	1.199	8906.3	0.010	≈100 (0.1-2; R) 250 (0.2-12; N) 240 (0.3-10; C) 12000 (20-100; I)
IGR J16388+3557	— —	4.5±0.5 [5.0±0.5]	— —	— —	0.675	4387.7	0.021	5100 (20-100; I)

Note: emission-line fluxes are reported both as observed and (between square brackets) corrected for the intervening Galactic absorption $E(B - V)_{Gal}$ along the object line of sight (from Schlegel et al. 1998). Line fluxes are in units of 10^{-15} erg cm^{-2} s^{-1} , whereas X-ray luminosities are in units of 10^{43} erg s^{-1} and the reference band (between round brackets) is expressed in keV.

In the last column, the upper-case letter indicates the satellite and/or the instrument with which the corresponding X-ray flux measurement was obtained (see text).

The typical error in the redshift measurement is ± 0.001 but for the spectrum of IGR J12319-0749, for which an uncertainty of ± 0.01 can be assumed.

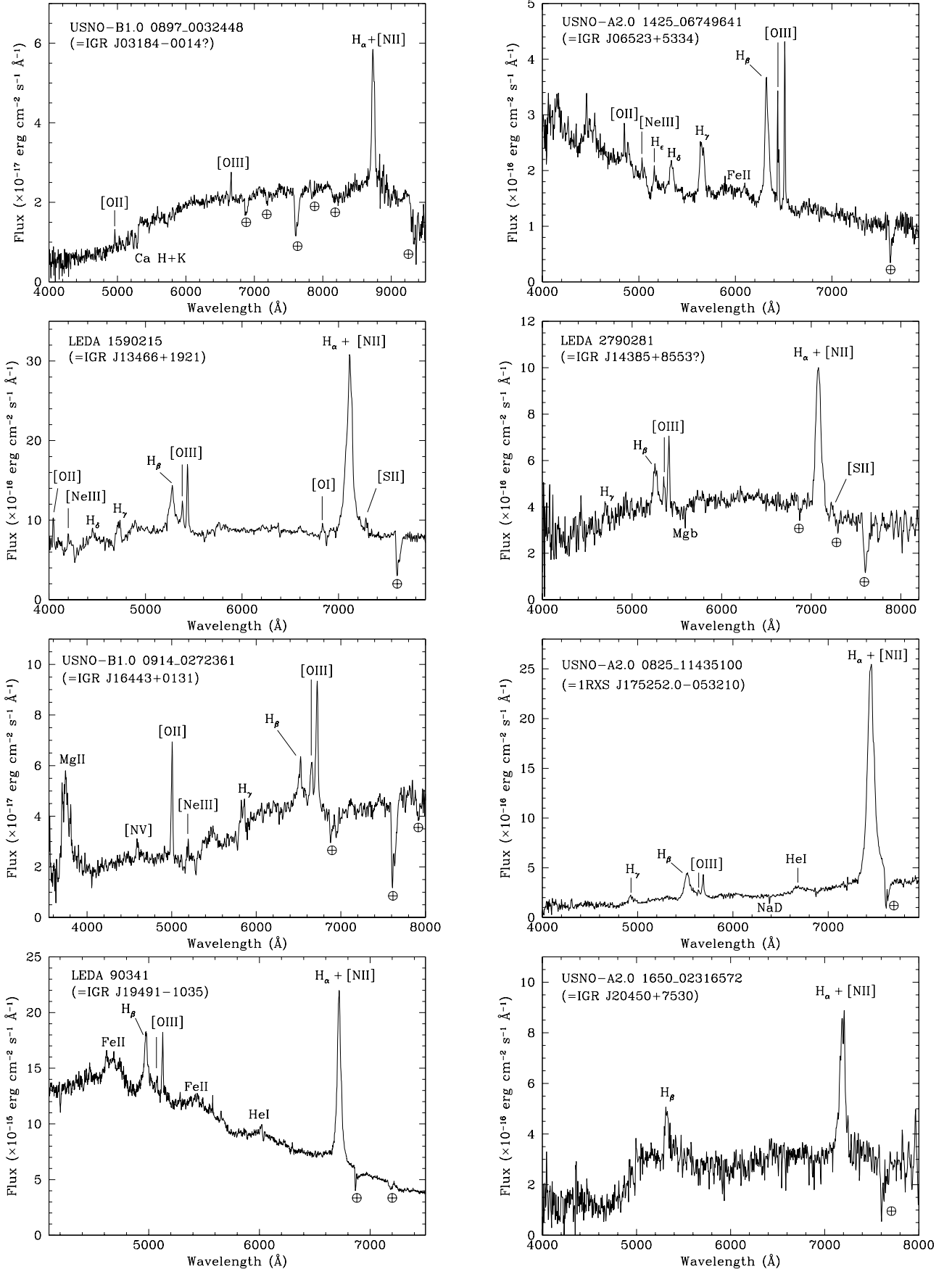


Fig. 4. Spectra (not corrected for the intervening Galactic absorption) of the optical counterparts of the 8 low-redshift, broad emission-line AGNs belonging to the sample of *INTEGRAL* sources presented in this paper. For each spectrum, the main spectral features are labeled. The symbol \oplus indicates atmospheric telluric absorption bands. The TNG spectrum has been smoothed using a Gaussian filter with $\sigma = 3 \text{ \AA}$.

Table 4. Synoptic table containing the main results for the 3 narrow emission-line AGNs (Fig. 6) identified or observed in the present sample of *INTEGRAL* sources.

Object	$F_{H\alpha}$	$F_{H\beta}$	$F_{[OIII]}$	Class	z	D_L (Mpc)	$E(B - V)$		L_X
							Gal.	AGN	
IGR J03249+4041									14 (14–150; <i>B</i>) 14 (14–195; <i>B</i>) 8.5 (17–60; <i>I</i>) 2.8 (0.2–12; <i>N</i>)
(LEDA 4678815)	30.4±1.5 [48±3]	3.9±0.6 [7.8±1.2]	27.2±1.4 [51±3]	Sy2	0.049	234.4	0.206	0.77	
(LEDA 97012)	29±3 [46±5]	1.3±0.3 [2.3±0.6]	17.3±1.2 [33±2]	Sy2	0.049	234.4	0.206	1.98	0.059 (0.2–12; <i>N</i>)
IGR J13550–7218	26±2 [56±5]	8.7±0.9 [25±4]	77±2 [218±7]	Sy2	0.071	345.0	0.360	0	3.0 (0.5–10; <i>X</i>) 21 (20–100; <i>I</i>)

Note: emission-line fluxes are reported both as observed and (between square brackets) corrected for the intervening Galactic absorption $E(B - V)_{Gal}$ along the object line of sight (from Schlegel et al. 1998). Line fluxes are in units of 10^{-15} erg cm $^{-2}$ s $^{-1}$, whereas X-ray luminosities are in units of 10^{43} erg s $^{-1}$ and the reference band (between round brackets) is expressed in keV. In the last column, the upper-case letter indicates the satellite and/or the instrument with which the corresponding X-ray flux measurement was obtained (see text).

culated an estimate of the mass of the central black hole in 13 of the 14 broad-line AGNs of our sample.

The corresponding black hole masses for these 13 cases are reported in Table 5. Here we assumed a null local absorption for all Type 1 AGNs. The main sources of error in these mass estimates generally come from the determination of the emission flux of the reference emission lines, which spans from 5% to 30% in our sample (see Tables 2 and 3), and from the scatter in the $R_{BLR} - L_{H\beta}$ scaling relation, which introduces typical uncertainties of 0.4–0.5 dex (i.e., logarithmic decimals) in the black hole mass estimate (Vestergaard 2004). As a whole, we expect the typical error to be about 50% of the value.

In Table 5 we also report the apparent Eddington ratios for the listed AGNs: these were obtained using the observed X-ray fluxes and/or upper limits in the 20–100 keV band. We considered this spectral range because, looking at Tables 2 and 3, all objects for which we could provide a black hole mass estimate have a flux measurement in this band and apparently they emit the bulk of their X-ray luminosity in this range. When needed, we rescaled the observed luminosities to the above spectral range assuming a photon index $\Gamma = 1.8$.

Although an in-depth study of these AGNs is beyond the scope of this paper, and more focused observations on these sources are needed to determine their physical properties such as broadband spectral energy distribution, Lorentz factor and true luminosity, one can see from Table 5 that the Eddington ratios can be around unity (or even more) for a number of these objects, especially for those at high redshift. This hints at an extreme blazar nature for them, as already found for various high- z objects detected or identified in hard X-ray surveys (see e.g. Bassani et al. 2007; Sambruna et al. 2007; Masetti et al. 2008b; Lanzuisi et al. 2011).

The properties of the high-redshift QSOs reported in Table 5 thus support the suggestion by Ghisellini et al. (2010, 2011) that the most powerful blazars have a spectral energy distribution with a high energy peak at MeV (or even lower) energies. This implies that the most extreme blazars can be found more efficiently in hard X-rays, rather than in the γ -ray band above the GeV threshold.

Table 5. BLR gas velocities (in km s $^{-1}$), central black hole masses (in units of $10^7 M_{\odot}$) and apparent Eddington ratios for 13 broad line AGNs belonging to the sample presented in this paper.

Object	v_{BLR}	M_{BH}	L_X/L_{Edd}
IGR J05255–0711	3000	15	<4.6
IGR J06523+5334	2000	3.6	<3.5
IGR J13466+1921	3800	4.6	~0.05
IGR J14385+8553	3000	1.7	<0.15
IGR J16443+0131	3700	4.3	<1.4
1RXS J175252.0–053210	3900	40	0.011
IGR J19491–1035	3400	3.2	~0.005
IGR J20450+7530	2700	2.4	<0.32
IGR J06073–0024	5300	50	<3.5
IGR J08262+4051	4200	15	<9.3
IGR J12562+2554	8400	90	1.1
IGR J16388+3557	23000	270	0.15
IGR J12319–0749	5600	280	<2.5

Note: the final uncertainties on the black hole mass estimates are about 50% of their values. The velocities were determined using $H\beta$, Mg II, or C IV emissions (upper, central and lower part of the table, respectively), whereas the apparent Eddington ratios were computed using the (observed or rescaled, see text) 20–100 keV luminosities.

4.2. Accreting binaries

Within our sample we identify 4 objects as Galactic accreting binaries. These are divided into the following subgroups: 2 dwarf nova CVs (RX J0525.3+2413 and AX J1740.2–2903), one symbiotic binary (IGR J17197–3010) and one HMXB (IGR J19173+0747).

4.2.1. CVs

The spectra of the objects identified as CVs (Fig. 7, upper panels) show characteristics typical of this class, such

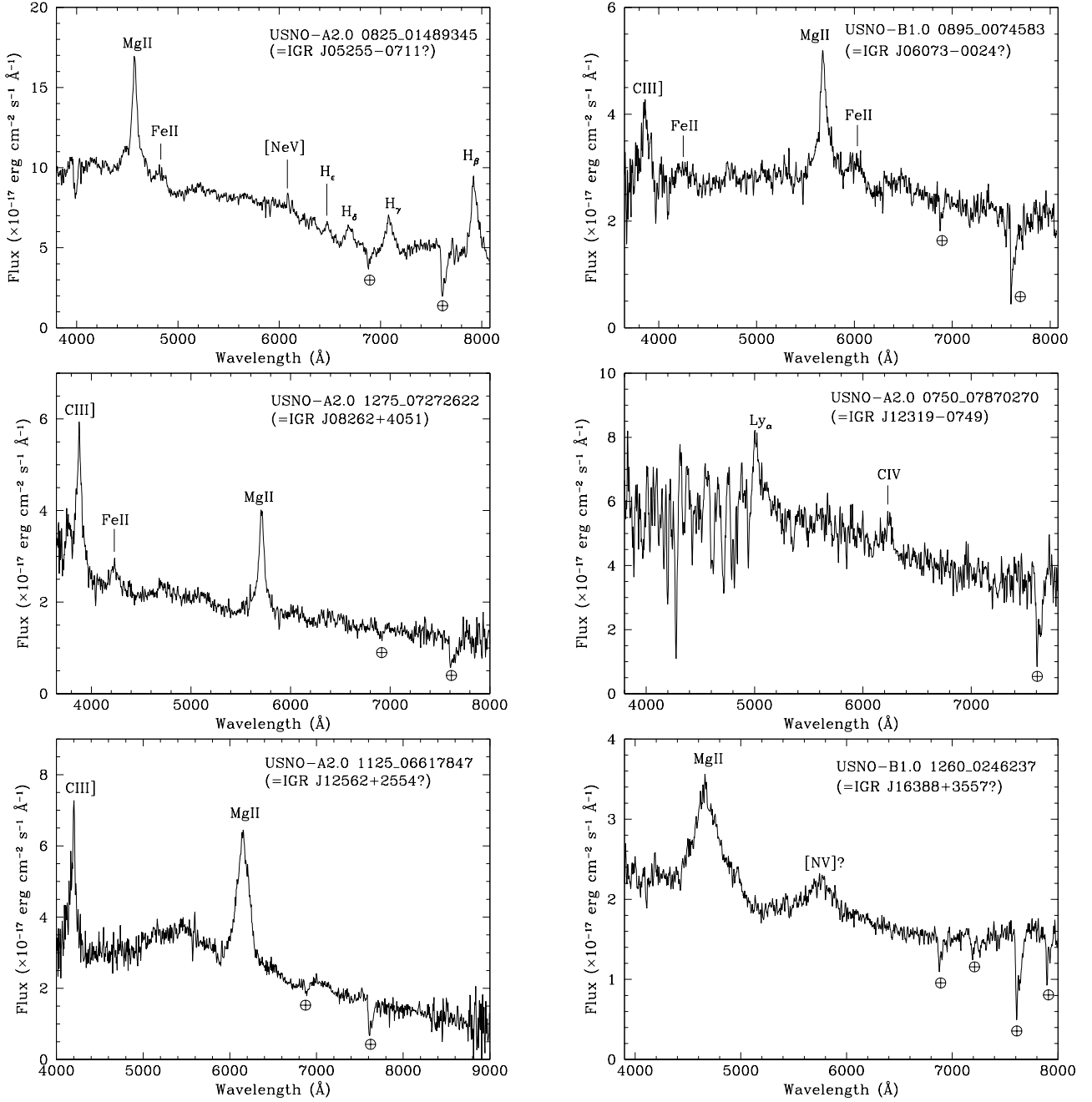


Fig. 5. Spectra (not corrected for the intervening Galactic absorption) of the optical counterparts of the 6 high-redshift QSOs belonging to the sample of *INTEGRAL* sources presented in this paper. For each spectrum, the main spectral features are labeled. The symbol \oplus indicates atmospheric telluric absorption bands. The TNG spectra have been smoothed using a Gaussian filter with $\sigma = 3 \text{ \AA}$.

as Balmer (up to H_δ in the case of RX J0525.3+2413) and helium lines in emission. All of these features lie at redshift $z = 0$, indicating that these sources are located within our Galaxy. Our results confirm the CV nature of sources RX J0525.3+2413 and AX J1740.2–2903 as first proposed by Torres et al. (2007) and Halpern & Gotthelf (2010), respectively.

The main spectral diagnostic lines of these objects, as well as the main astrophysical parameters which can be inferred from the available optical and X-ray observational

data, are given in Table 6. The X-ray luminosities listed in this table for the various objects were computed using the fluxes reported in Voges et al. (1999), Sidoli et al. (2001), Sakano et al. (2002), Saxton et al. (2008), Watson et al. (2009), Krivonos et al. (2010), Cusumano et al. (2010), Tueller et al. (2010), Page et al. (2007), Farrell et al. (2010) and Malizia et al. (2010).

In particular, source RX J0525.3+2413 shows an $\text{He II } \lambda 4686 / H_\beta$ equivalent width (EW) ratio which is larger than 1. As already suggested by Torres et al. (2007), this

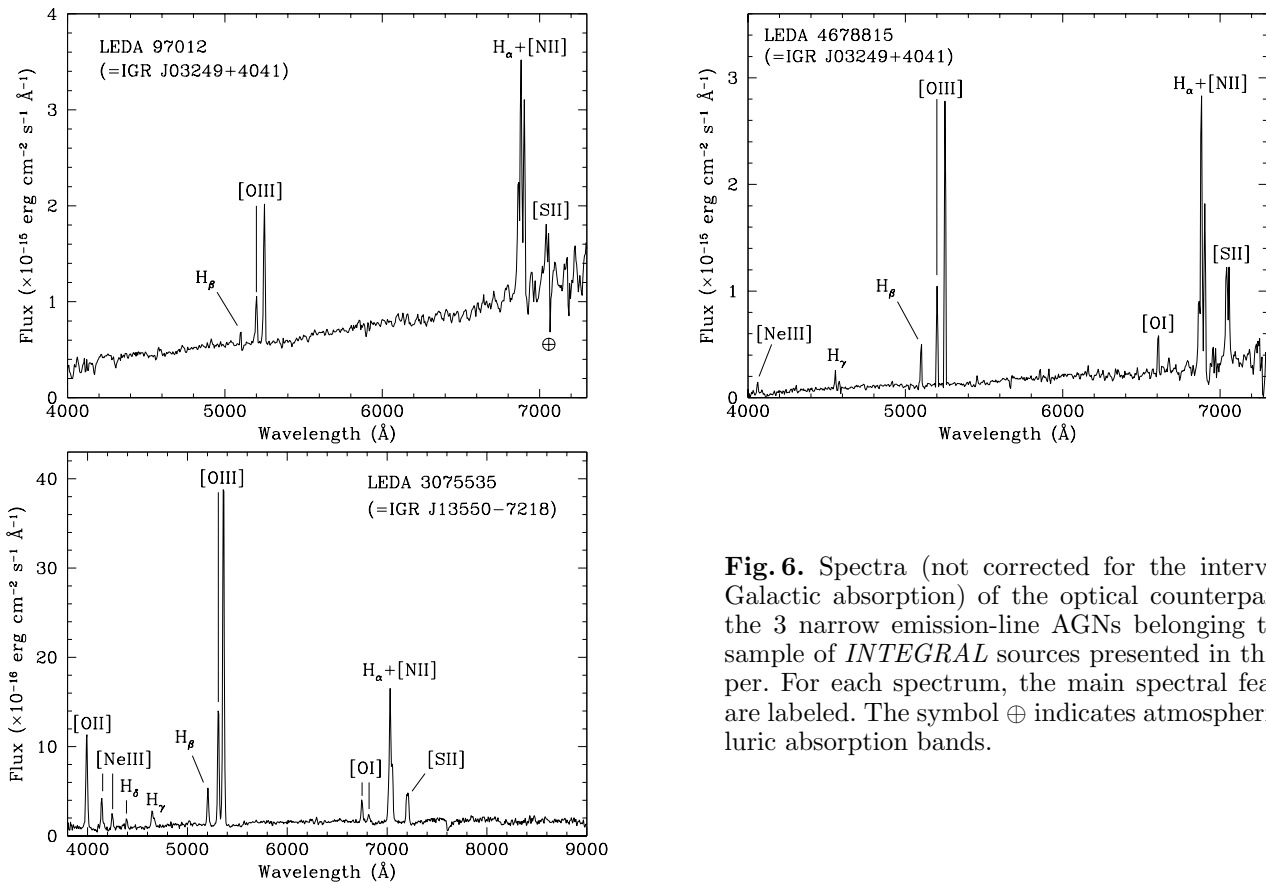


Fig. 6. Spectra (not corrected for the intervening Galactic absorption) of the optical counterparts of the 3 narrow emission-line AGNs belonging to the sample of *INTEGRAL* sources presented in this paper. For each spectrum, the main spectral features are labeled. The symbol \oplus indicates atmospheric telluric absorption bands.

supports the fact that this is likely a system hosting a strongly magnetized white dwarf (WD) and therefore possibly belonging to the “polar” subclass of CVs (see e.g. Cropper 1990). This classification however needs confirmation through the measurement of both the orbital period and the WD spin period, as optical spectroscopy is sometimes insufficient to firmly establish the magnetic nature of CVs (see e.g. Pretorius 2009 and de Martino et al. 2010).

We also note that the spectral continua of these two CVs appear substantially reddened. This may be explained by one (or more) of these possibilities: (i) they suffer from local absorption around the source; and/or (ii) they are substantially more distant from Earth than derived from their dereddened optical magnitudes because the actual magnitude of the sources is fainter than the one reported in the USNO-A2.0 catalog. The latter issue may be of some importance in the case of AX J1740.2–2903, for which Farrell et al. (2010) found 4 near-infrared objects within the *XMM-Newton* error circle: given the relatively low spatial resolution of the DSS images, some of them may possibly constitute a blend of sources in the USNO-A2.0 catalog, thus giving a counterpart magnitude brighter than the actual one for this object. Moreover, the USNO-A2.0 data can sometimes present systematic uncertainties of a few tenths of magnitude (see Masetti et al. 2003).

It may however be stressed that, for both CVs, the *V*-band absorption inferred from the optical spectra is substantially lower than the Galactic one along their direction (that is, ~ 2.7 and ~ 15 mag, respectively: see Schlegel et al. 1998), which may suggest that they do not in fact lie at

the other side of the Galaxy. As a confirmation of the reliability of this result of ours (at least for AX J1740.2–2903), we see that if we apply the empirical formula of Predehl & Schmitt (1995) to our estimate of the reddening along the source line of sight, we obtain a hydrogen column density $N_{\text{H}} = 6.2 \times 10^{21} \text{ cm}^{-2}$, which is a value broadly consistent with those obtained by Farrell et al. (2010) from the analysis of *XMM-Newton* X-ray data.

Again, concerning AX J1740.2–2903, we stress that its optical spectrum (upper right panel of Fig. 7) allows us to exclude the possibility that it is a Symbiotic X-ray binary as proposed by Farrell et al. (2010), because in this case the continuum typical of a late-type giant star with no emission lines would have clearly been detected (see e.g. Masetti et al. 2006e, 2007). We also take this opportunity to remark that the arcsec-sized X-ray position of this source reported by Malizia et al. (2010) suffers from a typo, and the correct one is reported in Halpern & Gotthelf (2010) and Farrell et al. (2010).

4.2.2. Symbiotic stars

As remarked previously, source IGR J17197–3010 is identified as a symbiotic star given its optical spectral continuum, which shows the typical features of a red giant star (namely, broad molecular bands) with superimposed H_{α} and H_{β} , H_{γ} and Ca II H+K emissions, again at $z = 0$ (Fig. 7, lower left panel).

Using the Bruzual-Persson-Gunn-Stryker (Gunn & Stryker 1983) and Jacoby-Hunter-Christian (Jacoby et al.

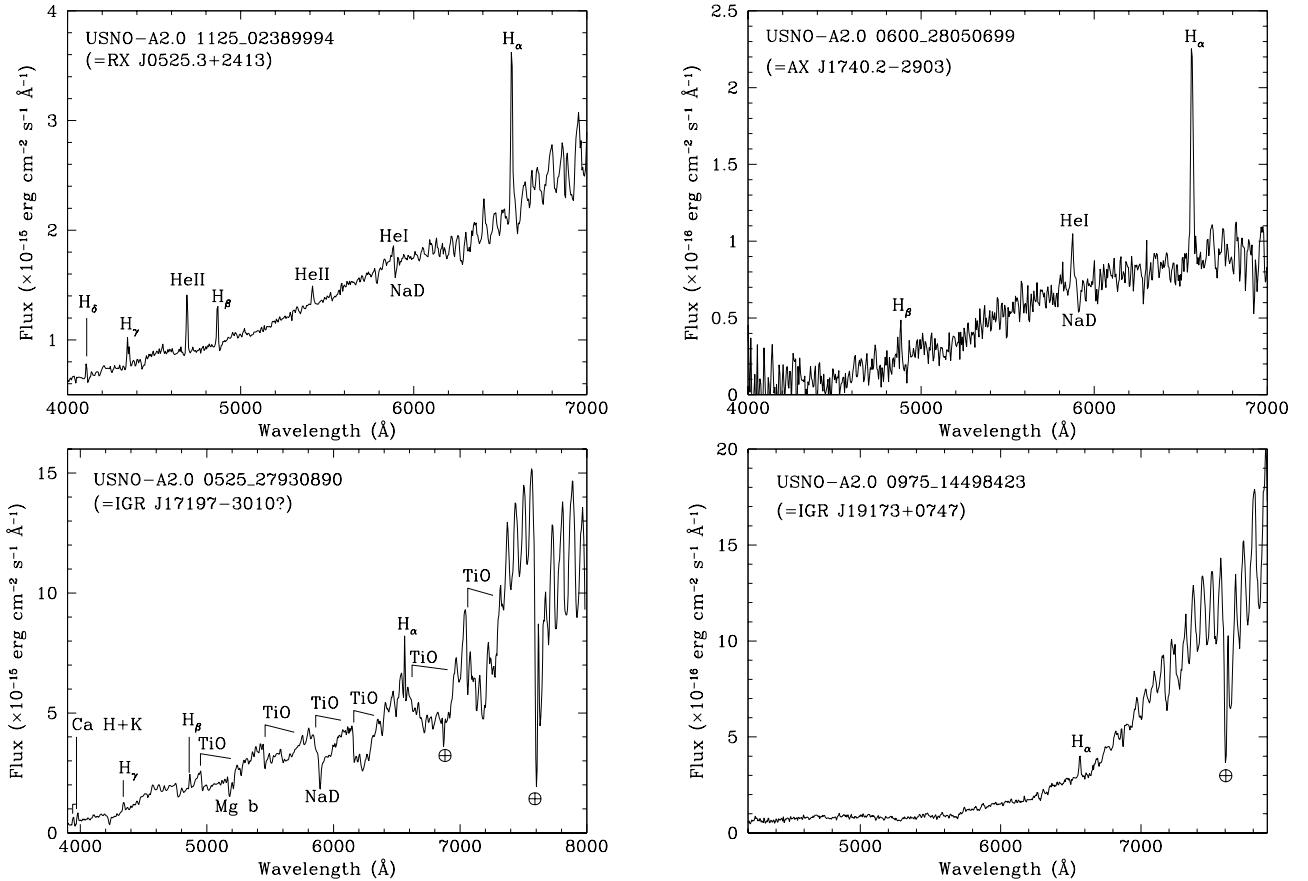


Fig. 7. Spectra (not corrected for the intervening Galactic absorption) of the optical counterparts of the 4 Galactic accreting binaries belonging to the sample of *INTEGRAL* sources presented in this paper. For each spectrum, the main spectral features are labeled. The symbol \oplus indicates atmospheric telluric absorption bands.

1984) spectroscopy atlases, we constrain the spectral type of the optical counterpart of this source as M1-2 III. We also note a possible excess on the blue side of the optical continuum, which is a common feature in symbiotic stars. From this spectral information, and assuming colours and absolute V magnitude of a M2 III star and considering the measured Balmer line ratio, we obtain a distance of ~ 16.6 kpc for the source, which would place it at the other side of the Galaxy.

This suggests that more absorption should occur along the line of sight and that this number should rather be used as an (admittedly loose) upper limit for the distance to this object. Indeed, if one assumes the total Galactic colour excess along the source line of sight, $E(B - V)_{\text{Gal}} = 1.051$ mag (Schlegel et al. 1998), we obtain a distance of ~ 6.3 kpc to the source.

4.2.3. HMXBs

We classified the object IGR J19173+0747 within our sample as an X-ray binary given the overall optical spectral shape and characteristics of an early-type star, which is typical of this class of objects (see Papers II-VIII). The lower right panel of Fig. 7 indeed shows that the object displays the H_{α} line in emission at redshift 0, superimposed on an intrinsically blue continuum modified by intervening

reddening: the latter is indicative of interstellar dust along its line of sight. This is quite common in X-ray binaries detected with *INTEGRAL* (e.g., Papers III-VIII) and indicates that the object lies relatively far from the Earth. From the optical magnitudes of IGR J19173+0747 we however find a V -band reddening about 2 mag lower than the Galactic one along its line of sight ($A_V \sim 6.1$; Schlegel et al. 1998).

Table 7 collects the relevant optical spectral information about this source, along with the main parameters inferred from the available X-ray and optical data. X-ray luminosities in Table 7 were calculated using the fluxes in Voges et al. (2000) and Pavan et al. (2011). We obtained constraints on distance, reddening, spectral type, and X-ray luminosity shown in the table by considering the absolute magnitudes of early-type stars and by applying the method described in Papers III and IV for the classification of this type of X-ray sources. In particular, we exclude the possibility that the source is of luminosity class I or III otherwise it would be placed well beyond the Galactic disk (>30 kpc from Earth). The lack of further detailed photometric optical information and of higher-resolution spectroscopy does not allow us to further refine our spectral classification for this object.

In addition, using the empirical formula of Predehl & Schmitt (1995) to obtain the hydrogen column value from

Table 6. Synoptic table containing the main results concerning the 2 CVs (in the upper part) and of the symbiotic star (in the lower part) identified in the present sample of *INTEGRAL* sources (see Fig. 7).

Object	H_α		H_β		$\text{He II } \lambda 4686$		R mag	A_V (mag)	d (pc)	L_X
	EW	Flux	EW	Flux	EW	Flux				
RX J0525.3+2413	8.0 ± 0.9	18 ± 2	4.0 ± 0.4	3.8 ± 0.4	6.1 ± 0.6	5.4 ± 0.5	15.6	1.6	~ 110	0.10 (0.1–2.4; <i>R</i>) 1.1 (0.2–12; <i>N</i>) 1.5 (0.3–10; <i>X</i>) 1.7 (17–60; <i>I</i>) 3.0 (14–150; <i>B</i>) 2.5 (14–195; <i>B</i>)
AX J1740.2–2903	31 ± 3	2.6 ± 0.3	15 ± 5	0.3 ± 0.1	< 40	< 0.3	17.4	3.46	~ 130	0.67 (0.1–2.4; <i>R</i>) 0.80 (0.2–10; <i>N</i>) 0.99 (0.7–10; <i>A</i>) 0.77 (0.2–12; <i>N</i>) 0.65 (2–10; <i>X</i>) 1.4 (20–100; <i>I</i>)
IGR J17197–3010	4.5 ± 0.5	27 ± 3	3.8 ± 0.6	7.6 ± 1.1	< 1.8	< 3.0	14.8	0.726	$\lesssim 16600$	$\lesssim 16000$ (17–60; <i>I</i>)

Note: EWs are expressed in Å, line fluxes are in units of 10^{-15} erg cm $^{-2}$ s $^{-1}$, whereas X-ray luminosities are in units of 10^{31} erg s $^{-1}$ and the reference band (between round brackets) is expressed in keV.
In the last column, the upper-case letter indicates the satellite and/or the instrument with which the corresponding X-ray flux measurement was obtained (see text).

our reddening determination, we find $N_H \approx 7 \times 10^{21}$ cm $^{-2}$; this is slightly higher than the upper limit ($< 6 \times 10^{21}$ cm $^{-2}$) obtained by Pavan et al. (2011) for this source; however, given the large uncertainties affecting the measurements involved in our calculation, we can consider the two values as basically compatible with each other.

We finally note that this system has no known radio source associated. This implies that it is an X-ray binary that does not display collimated (jet-like) outflows, that is, it has not the characteristics of a microquasar.

4.3. Other Galactic objects

Two of the selected sources, IGR J18371+2634 and IGR J23130+8608, display a star-like continuum typical of late-G/early-K type stars, with a faint but statistically significant H_α emission at $z = 0$ (see Fig. 8, upper panels). This optical spectral appearance is very similar to that of source IGR J08023–6924, tentatively identified as a RS CVn star (Paper VI; Rodriguez et al. 2010a). We thus suggest a chromospherically active star identification for these two sources as well.

The main observed and inferred parameters for each object are reported in Table 8. Luminosities are computed using the X-ray fluxes reported in Voges et al. (2000), Bird et al. (2007, 2010), Rodriguez et al. (2010a) and Landi et al. (2011).

Assuming, as stated at the beginning of Section 4, that these two objects are similar to the active star II Peg — which has magnitude $R \sim 6.9$ (Monet et al. 2003) and for which we determine a distance of 40 pc from Earth based on its measured parallax of 25.06 milliarcsec (van Leeuwen 2007) — we obtain the distances reported in Table 8. We stress that these figures should be considered as upper limits, as no reddening correction on the observed magnitudes of the optical counterparts of IGR J18371+2634 and IGR J23130+8608 was attempted.

We point out that the counterpart of IGR J18371+2634 mentioned above is source #1 of Landi et al. (2011); this

is the northern source indicated in the upper right panel of Fig. 3. We note that we also acquired a spectrum of source #2 (that is, the southern one in the upper right panel of Fig. 3) simultaneously with the one of source #1. This spectrum is reported in Fig. 8 (lower left panel): its appearance is typical of a symbiotic star, similar to that of the optical counterpart of IGR J17197–3010 (see Section 3.2). However, given its position with respect to the IBIS error circle and the non-detection of X-ray flux above 2 keV from it (Landi et al. 2011), we consider this object as an unlikely counterpart to the X-ray source IGR J18371+2634, although one cannot exclude a sporadic contribution of this symbiotic star to the hard X-ray emission detected with *INTEGRAL*.

Of course, a deeper multiwavelength followup is needed to confirm (or disprove) the two tentative active star identifications above.

4.4. Statistics

As is customary for our set of papers, we here present an update of the statistics in our previous works by adding the results from the sample presented here as well as those reported in Bikmaev et al. (2010), Corbet et al. (2010), Pellizza et al. (2011) and Maiorano et al. (2011).

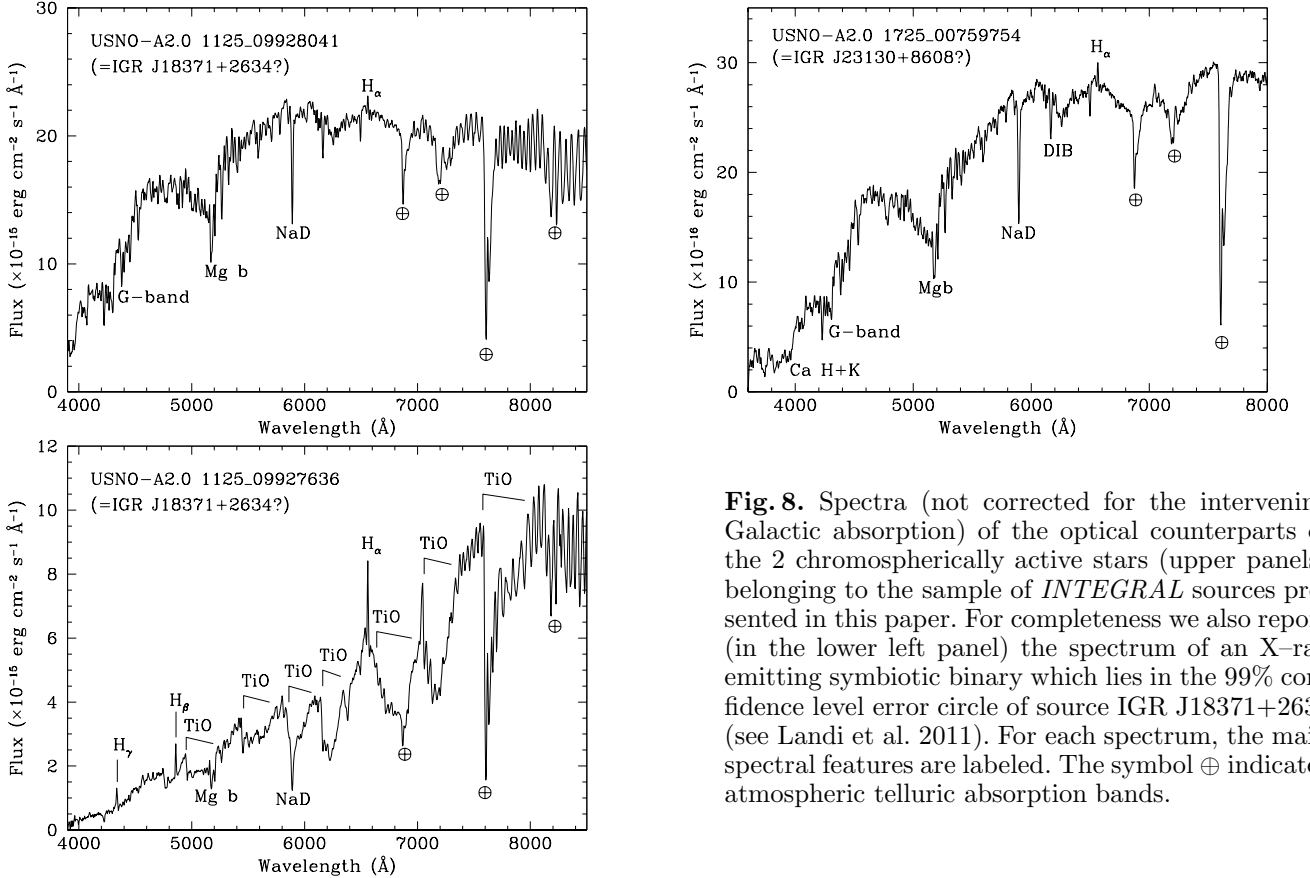
We find that the 204 *INTEGRAL* sources identified up until now, on the basis of their optical or NIR spectroscopy, are distributed in the following manner into the main broad classes discussed in Papers VI–VIII and in this one: 125 (61.2%) are AGNs, 51 (25.0%) are X-ray binaries, 25 (12.3%) are CVs, and 3 cases (1.5%) possibly belong to the class of active stars.

When we consider the AGN subclasses, we see that 62 sources (i.e., 50% of the AGN identifications) are Seyfert 1 galaxies, 46 (37%) are narrow-line AGNs (including 43 Seyfert 2 galaxies and 3 LINERS), while the QSO, XBONG, and BL Lac subclasses are populated by 10, 4, and 3 objects (8%, 3%, and 2%), respectively (see e.g. Paper VIII and

Table 7. Main results for the HMXB IGR J19173+0747 (see Fig. 7, lower right panel) identified in the present sample of *INTEGRAL* sources.

Object	H_{α}		H_{β}		$He II \lambda 4686$		R mag	A_V (mag)	d (kpc)	Spectral type	L_X
	EW	Flux	EW	Flux	EW	Flux					
IGR J19173+0747	6.1 ± 0.6	1.77 ± 0.18	<10	<0.8	<10	<0.8	16.0	~ 4.2	~ 10	early B V	0.027 (0.1–2.4; <i>R</i>) 0.72 (0.5–10; <i>X</i>) 0.67 (20–40; <i>I</i>)

Note: EWs are expressed in Å, line fluxes are in units of 10^{-15} erg cm^{-2} s^{-1} , whereas X-ray luminosities are in units of 10^{35} erg s^{-1} and the reference band (between round brackets) is expressed in keV.
In the last column, the upper-case letter indicates the satellite and/or the instrument with which the corresponding X-ray flux measurement was obtained (see text).

**Fig. 8.** Spectra (not corrected for the intervening Galactic absorption) of the optical counterparts of the 2 chromospherically active stars (upper panels) belonging to the sample of *INTEGRAL* sources presented in this paper. For completeness we also report (in the lower left panel) the spectrum of an X-ray emitting symbiotic binary which lies in the 99% confidence level error circle of source IGR J18371+2634 (see Landi et al. 2011). For each spectrum, the main spectral features are labeled. The symbol \oplus indicates atmospheric telluric absorption bands.

references therein for an explanation of the properties of these latter subclasses).

For the Galactic objects, it is found that 40 and 11 objects (78% and 22% of the X-ray binary identifications) are HMXBs and LMXBs, respectively; in addition, 25 sources are classified as CVs, most of which (20, that is 80% of them) are definite or likely dwarf novae (mostly of magnetic type), and the remaining 5 are symbiotic stars.

When we compare the above figures with those of our previous papers, we see no substantial changes in the source distribution among the various classes, as the main group is made of AGN, followed by X-ray binaries and CVs. It is apparent from the identification results presented in this paper that the approach used in our program, that is, the use of optical spectroscopy to pinpoint the nature of *INTEGRAL* sources strongly favours the discovery of

AGNs against the other classes of objects. Moreover, the use of medium-sized and large telescopes (as TNG and GTC, in the present case), allows us to study the faint end of the distribution of putative optical counterparts of these high-energy sources.

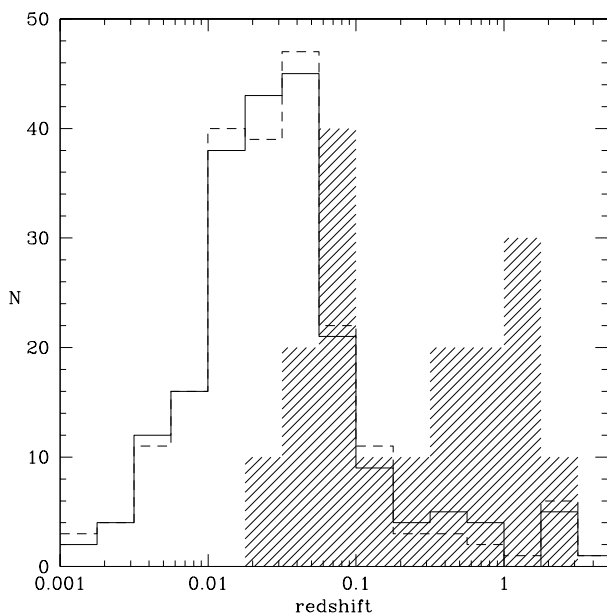
With regards to this issue, we note that the average redshift of the AGNs in the sample of the present paper is $\langle z \rangle = 0.576$. This can be compared e.g. with the average redshift ($\langle z \rangle = 0.135$) of the known extragalactic sources from the 4th IBIS survey (Bird et al. 2010); likewise, the value of the same parameter in the catalog of Krivonos et al. (2010) is $\langle z \rangle = 0.144$.

This is graphically apparent in Fig. 9, where the logarithmic histograms of the redshift distribution of the known AGNs in the surveys of Bird et al. (2010) and Krivonos et al. (2010) are plotted together with that of the AGN identi-

Table 8. Synoptic table containing the main results for the active stars (see Fig. 8) identified in the present sample of *INTEGRAL* sources.

Object	H_{α}		R mag	d (pc)	L_X
	EW	Flux			
IGR J18371+2634(#1)	0.59 ± 0.12	13 ± 3	12.5	530	0.0057 (0.1–2.4; <i>R</i>) 0.0044 (2–10; <i>X</i>) 0.47 (20–40; <i>I</i>) <0.47 (40–100; <i>I</i>)
IGR J23130+8608	0.74 ± 0.07	2.1 ± 0.2	14.7	1500	0.019 (2–10; <i>X</i>) 3.8 (20–40; <i>I</i>) <4.6 (40–100; <i>I</i>)

Note: EWs are expressed in Å, line fluxes are in units of 10^{-15} erg cm $^{-2}$ s $^{-1}$, whereas X-ray luminosities are in units of 10^{33} erg s $^{-1}$ and the reference band (between round brackets) is expressed in keV. In the last column, the upper-case letter indicates the satellite and/or the instrument with which the corresponding X-ray flux measurement was obtained (see text).

**Fig. 9.** Logarithmic histograms showing the frequency of known AGN redshifts in the surveys of Bird et al. (2010; continuous line) and of Krivonos et al. (2010; dashed line), together with the logarithmic distribution of redshifts of AGNs identified in the present paper (shaded histogram; note that for this latter case the actual numbers are multiplied by 10 for the sake of comparison).

fied in this paper (the numbers of the latter one have been multiplied by 10 in Fig. 9 to ease the comparison by eye). All histograms have binning of 0.25 dex. One can see that, while the redshift distributions of known AGNs in the two mentioned *INTEGRAL* surveys are similar to each other and are dominated by nearby objects (with $z < 0.05$), that of the present sample has substantially different shape and range: indeed, two peaks (one around $z \sim 0.1$ and the other at $z \sim 1$) are present, and no object with $z < 0.02$ is found.

To quantify this difference between the redshift distribution of the present sample and those of Bird et al. (2010) and Krivonos et al. (2010), we applied a Kolmogorov-

Smirnov nonparametric test (e.g., Kirkman 1996): we found that the probability that the redshift distribution of the present sample and those of known AGNs in either of the two above catalogs is less than 0.001 in both cases. This confirms that the AGNs of the present sample are drawn from a different distribution, of more distant objects, with respect to that of known AGNs in both Bird et al. (2010) and Krivonos et al. (2010).

The above considerations thus indicate that the deeper *INTEGRAL* observations available with the latest surveys allow one to explore the hard X-ray emitting sources in the far universe, at a mean distance ~ 5 times larger than that of the average of such type of objects known up to now.

As a final comment, one may wonder whether there is a physical reason behind the bimodal distribution of the redshifts of the newly-identified AGNs in the present sample, as shown in Fig. 9. Specifically, are we looking at two different physical classes of AGNs in the nearby and distant universe, or rather is it just a selection effect due to the merging of a wide-field, shallow survey with a series of narrow-field, deeper pointed observations? Although the possibility of a selection bias of this kind, together with an effect of small-number statistics, cannot be excluded *a priori*, we think that (as stressed at the end of Section 4.1) the high- z sources are indeed different from the other ones at lower redshift in the sense that they belong to a subclass of extreme blazars which emit the bulk of their power in the hard X-ray band; thus, they begin to be detected by wide-field surveys when a deep enough level of sensitivity is reached.

5. Conclusions

Continuing our ongoing identification program of *INTEGRAL* sources by means of optical spectroscopy (Papers I–VIII) pursued using various telescopes since 2004, we have identified and studied 22 objects having unknown or poorly explored nature and belonging to surveys of the hard X-ray sky (Bird et al. 2010; Krivonos et al. 2010; Pavan et al. 2011). This has been made possible by using 6 telescopes of different sizes (from 1.5 to 10.4 metres of aperture) and archival data from one spectroscopic survey.

We found that the selected sample largely consists of AGNs; indeed, 16 sources belong to this class: 14 are of

Type 1 (6 of them lie at high redshift, having $z > 0.5$) and 2 are of Type 2 (one of which is a system of two interacting Seyfert 2 galaxies). The other objects belong to our Galaxy: we found that two of them are (probably magnetic) CVs, one is a HMXB, one is a symbiotic star, and two are possibly identified as active stars.

These findings confirm the absolute majority of AGNs among our identification program. Moreover, the observations presented here allowed us to increase by more than a factor of two the number of hard X-ray emitting high-redshift AGNs discovered through optical spectroscopy, and to discover and identify the source IGR J12319–0749 (with redshift $z = 3.12$) as the second farthest persistently emitting hard X-ray object within the *INTEGRAL* catalogs. Our black hole mass estimates for these high- z AGNs also support the fact that hard X-ray surveys may efficiently spot extremely powerful blazars in the distant Universe.

This identification program has also been proven to be of great importance in the detection of highly absorbed (and even Compton-thick) active galaxies, especially in the local Universe. This is fundamental for the estimate of their fraction among the AGN population (see Malizia et al. 2009 and Burlon et al. 2011); moreover, with the detections in the present work, this project may also start helping to resolve the hard X-ray background, or at least to evaluate the relative contribution of high- z sources detected and identified in this spectral range.

All of this has been possible through the combined use of the recently published deep *INTEGRAL* surveys and of large telescopes, such as the most powerful ones used in this paper.

It is moreover stressed that 173 of the 204 optical and NIR spectroscopic identifications considered in Section 4.4 (that is, nearly 85%) were obtained or refined within the framework of our spectroscopic follow-up program originally started in 2004 (Papers I–VIII, the present work, and references therein).

The results presented here once again demonstrate the high effectiveness of the method of catalog cross-correlation and/or follow-up observations (especially with soft X-ray satellites capable of providing arcsec-sized error boxes, such as *Chandra*, *XMM-Newton* or *Swift*), and optical spectroscopy to determine the actual nature of still unidentified or poorly known *INTEGRAL* sources. We however recall that, for 8 objects of our present sample, only a putative albeit likely optical counterpart could be identified because it lies in the 99% confidence level error circle of the corresponding hard X-ray source, or because of the lack of soft X-ray observations providing a definite arcsec-sized position at high energies. In the latter case, timely observations with soft X-ray satellites affording arcsec-sized localizations are needed to confirm the proposed association.

Present and future surveys at optical and NIR wavelengths, such as the ongoing Vista Variables in the Vía Láctea (VVV: Minniti et al. 2010; Saito et al. 2011) public NIR survey, will permit us to check and identify variable objects in the fields of the objects detected in published and forthcoming *INTEGRAL* catalogs, thus easing the search for putative counterparts for these high-energy sources. Indeed, this approach has already been tested to search for the quiescent NIR counterpart of hard X-ray transients detected with *INTEGRAL*, providing encouraging results and allowing one to place constraints on the

nature of these objects (Rojas et al. 2011; Greiss et al. 2011a,b).

Acknowledgements. We thank Silvia Galletti for Service Mode observations at the Loiano telescope, and Roberto Gualandi and Ivan Bruni for night assistance; Giorgio Martorana and Mauro Rebeschini for Service Mode observations at the Asiago telescope and Luciano Traverso for coordinating them; Aldo Fiorenzano for Service Mode observations at the TNG; Manuel Hernández for Service Mode observations at the CTIO telescope and Fred Walter for coordinating them. NM thanks Sean Farrell for useful discussions. We also thank the anonymous referee for useful remarks which helped us to improve the quality of this paper. This research has made use of the ASI Science Data Center Multimission Archive; it also used the NASA Astrophysics Data System Abstract Service, the NASA/IPAC Extragalactic Database (NED), and the NASA/IPAC Infrared Science Archive, which are operated by the Jet Propulsion Laboratory, California Institute of Technology, under contract with the National Aeronautics and Space Administration. This publication made use of data products from the Two Micron All Sky Survey (2MASS), which is a joint project of the University of Massachusetts and the Infrared Processing and Analysis Center/California Institute of Technology, funded by the National Aeronautics and Space Administration and the National Science Foundation. This research has also made use of data extracted from the Six-degree Field Galaxy Survey archive; it has also made use of the SIMBAD and VIZIER database operated at CDS, Strasbourg, France, and of the HyperLeda catalog operated at the Observatoire de Lyon, France. NM acknowledges ASI-INAF financial support via grant No. I/009/10/0 and thanks the Departamento de Astronomía y Astrofísica of the Pontificia Universidad Católica de Chile in Santiago for the warm hospitality during the preparation of this paper. PP has been supported by the ASI-INTEGRAL grant No. I/008/07. RL is supported by the ASI-INAF agreement No. I/033/10/0. LM is supported by the University of Padua through grant No. CPS0204. VC is supported by the CONACyT research grants 54480 and 15149 (México). DM is supported by the Basal CATA PFB 06/09, and FONDAF Center for Astrophysics grant No. 15010003. GG is supported by Fondecyt grant No. 1085267.

References

- Assafin, M., Andrei, A.H., Vieira Martins, R., et al. 2001, *ApJ*, 552, 380
- Bassani, L., Dadina, M., Maiolino, R., et al. 1999, *ApJS*, 121, 473
- Bassani, L., Landi, R., Malizia, A., et al. 2007, *ApJ*, 669, L1
- Bianchi, S., Corral, A., Panessa, F., et al. 2008, *MNRAS*, 385, 195
- Bikmaev, I., Irtuganov, E., Sakhbullin, E., et al. 2010, *ATel* #3072
- Bird, A.J., Malizia, A., Bazzano, A., et al. 2007, *ApJS*, 170, 175
- Bird, A.J., Bazzano, A., Hill, A.B., et al. 2009, *MNRAS*, 393, L11
- Bird, A.J., Bazzano, A., Bassani, L., et al. 2010, *ApJS*, 186, 1
- Burlon D., Ajello, M., Greiner, J., et al. 2011, *ApJ*, 728, 58
- Cardelli, J.A., Clayton, G.C., & Mathis, J.S. 1989, *ApJ*, 345, 245
- Chenevez, J., Falanga, M., Kuulkers, E., et al. 2007, *A&A*, 469, L27
- Condon, J.J., Cotton, W.D., Greisen, E.W., et al. 1998, *AJ*, 115, 1693
- Corbet R.H.D., Krimm, H.A., Barthelmy, S.D., et al. 2010, *ATel* #2570
- Cropper, M. 1990, *Space Sci. Rev.*, 54, 195
- Cusumano, G., La Parola, V., Segreto, A., et al. 2010, *A&A*, 524, A64
- de Martino, D., Falanga, M., Bonnet-Bidaud, J.-M., et al. 2010, *A&A*, 515, A25
- Del Santo, M., Sidoli, L., Mereghetti, S., et al. 2007, *A&A*, 468, L17
- Deutsch, E.W. 1999, *AJ*, 118, 1882
- Ducati, J.R., Bevilacqua, C.M., Rembold, S.B., & Ribeiro, D. 2001, *ApJ*, 558, 309
- Farrell, S.A., Gosling, A.J., Webb, N.A., et al. 2010, *A&A*, 523, A50
- Fiocchi, M., Bassani, L., Bazzano, A., et al. 2010, *ApJ*, 720, 987
- Ghisellini, G., Della Ceca, R., Volonteri, M., et al. 2010, *MNRAS*, 405, 387
- Ghisellini, G., Tagliaferri, G., Foschini, L., et al. 2011, *MNRAS*, 411, 901
- Greiss, S., Steeghs, D., Maccarone, T., et al. 2011a, *ATel* #3562
- Greiss, S., Steeghs, D., Maccarone, T., et al. 2011b, *ATel* #3688
- Gunn, J.E., & Stryker, L.L. 1983, *ApJS*, 52, 121
- Halpern, J.P., 2011, *ATel* #3186
- Halpern, J.P., & Gotthelf, E.V. 2010, *ATel* #2664
- Ho, L.C., Filippenko, A.V., & Sargent, W.L.W. 1993, *ApJ*, 417, 63
- Ho, L.C., Filippenko, A.V., & Sargent, W.L.W. 1997, *ApJS*, 112, 315

- Horne, K. 1986, *PASP*, 98, 609
- Jacoby, G.H., Hunter, D.A., & Christian, C.A. 1984, *ApJS*, 56, 257
- Jones, D.H., Saunders, W., Colless, M., et al. 2004, *MNRAS*, 355, 747
- Jones, D.H., Saunders, W., Read, M., Colless, M. 2005, *PASA*, 22, 277
- Kaspi, S., Smith, P.S., Netzer, H., et al. 2000, *ApJ*, 533, 631
- Kauffmann, G., Heckman, T.M., Tremonti, C., et al. 2003, *MNRAS*, 346, 1055
- Kirkman, T.W. 1996, *Statistics to Use* (<http://www.physics.csbsju.edu/stats/>)
- Krivosos, R., Tsygankov, S., Revnivtsev, M., et al. 2010, *A&A*, 523, A61
- Krivosos, R., Tsygankov, S., Burenin, R., Revnivtsev, M., & Lutovinov, A. 2011, *ATel* #3382
- La Parola, V., Cusumano, G., Romano, P., et al. 2010, *MNRAS*, 405, L66
- Landi, R., Maiorano, E., Fiocchi M., et al. 2010a, *ATel* #2731
- Landi, R., Bassani, L., Malizia, A., et al. 2010b, *ATel* #2830
- Landi, R., Malizia, A., Bazzano, A., et al. 2010c, *ATel* #3078
- Landi, R., Bassani, L., Bazzano, A., et al. 2010d, *ATel* #2563
- Landi, R., Malizia, A., Bazzano, A., et al. 2011, *ATel* #3185
- Lang, K.R. 1992, *Astrophysical Data: Planets and Stars*. Springer-Verlag, New York
- Lanzuisi, G., De Rosa, A., Ghisellini, G., et al. 2011, *MNRAS*, in press [[arXiv:1112.0472](http://arxiv.org/abs/1112.0472)]
- Lutovinov, A., Burenin, R., Sazonov, S., et al. 2010, *ATel* #2759
- Maiorano, E., Landi, R., Stephen, J.B., et al. 2011, *MNRAS*, 416, 531
- Malizia, A., Landi, R., Bassani, L., et al. 2007, *ApJ*, 668, 81
- Malizia, A., Stephen, J.B., Bassani, L., et al. 2009, *MNRAS*, 399, 944
- Malizia, A., Bassani, L., Sguera, V., et al. 2010, *MNRAS*, 408, 975
- Masetti, N., & Schiavone, F. 2008, *IASF-Bologna Internal Report No. 522/2008*
- Masetti N., Palazzi, E., Pian, E., et al. 2003, *A&A*, 404, 465
- Masetti, N., Palazzi, E., Bassani, L., Malizia, A., & Stephen, J.B. 2004, *A&A*, 426, L41 (Paper I)
- Masetti, N., Mason, E., Bassani, L., et al. 2006a, *A&A*, 448, 547 (Paper II)
- Masetti, N., Pretorius, M.L., Palazzi, E., et al. 2006b, *A&A*, 449, 1139 (Paper III)
- Masetti, N., Bassani, L., Bazzano, A., et al. 2006c, *A&A*, 455, 11 (Paper IV)
- Masetti, N., Morelli, L., Palazzi, E., et al. 2006d, *A&A*, 459, 21 (Paper V)
- Masetti N., Orlandini, M., Palazzi, E., Amati, L., & Frontera, F. 2006e, *A&A*, 453, 295
- Masetti, N., Landi, R., Pretorius, M.L., et al. 2007, *A&A*, 470, 331
- Masetti, N., Mason, E., Morelli, L., et al. 2008a, *A&A*, 482, 113 (Paper VI)
- Masetti, N., Mason, E., Landi, R., et al. 2008b, *A&A*, 480, 715
- Masetti, N., Parisi, P., Palazzi, E., et al. 2009, *A&A*, 495, 121 (Paper VII)
- Masetti, N., Parisi, P., Palazzi, E., et al. 2010, *A&A*, 519, A96 (Paper VIII)
- Masetti, N., Parisi, P., Jiménez-Bailón, E., et al. 2011, The nature of 19 X-ray sources detected with *INTEGRAL*. In: Proc. of Conference “The Extreme and Variable High Energy Sky”, Proc. of Science, SISSA, in press [[arXiv:1112.0318](http://arxiv.org/abs/1112.0318)]
- Mauch, T., Murphy, T., Buttery, H.J., et al. 2003, *MNRAS*, 342, 1117
- McLure, R.J., & Jarvis, M.J. 2002, *MNRAS*, 337, 109
- Minniti, D., Lucas, P.W., Emerson, J.P., et al. 2010, *New Astronomy*, 15, 433
- Monet, D.G., Levine, S.E., Canzian, B., et al. 2003, *AJ*, 125, 984
- Murphy, T., Mauch, T., Green, A., et al. 2007, *MNRAS*, 382, 382
- Osterbrock, D.E. 1989, *Astrophysics of Gaseous Nebulae and Active Galactic Nuclei* (Mill Valley: Univ. Science Books)
- Page, K.L., Tueller, J., & Beardmore, A.P. 2007, *ATel* #1279
- Panessa, F., & Bassani, L. 2002, *A&A*, 394, 435
- Parisi, P., Masetti, N., Landi, R., et al. 2010, *ATel* #2839
- Pavan, L., Bozzo, E., Ferrigno, C., et al. 2011, *A&A*, 526, A122
- Pellizza, L.J., Chaty, S., & Chisari, N.E. 2011, *A&A*, 526, A15
- Predehl, P., & Schmitt, J.H.M.M. 1995, *A&A*, 293, 889
- Pretorius, M.L. 2009, *MNRAS*, 395, 386
- Rodriguez, J., Tomsick, J.A., & Bodaghee, A. 2010a, *A&A*, 517, A14
- Rodriguez, J., Bodaghee, A., & Tomsick, J.A. 2010b, *ATel* #2557
- Rojas, A., Masetti, N., & Minniti, D., 2011, *ATel* #3275
- ROSAT* Team 2000, *ROSAT News No. 71*
- Sakano, M., Koyama, K., Murakami, H., Maeda, Y., & Yamauchi, S. 2002, *ApJS*, 138, 19
- Saito, R.K., Hempel, M., Minniti, D. et al. 2011, *A&A*, in press [[arXiv:1111.5511](http://arxiv.org/abs/1111.5511)]
- Sambruna, R.M., Tavecchio, F., Ghisellini, G. et al. 2007, *ApJ*, 669, 884
- Saxton R.D., Read, A.M., Esquej, P., et al. 2008, *A&A*, 480, 611
- Schlegel, D.J., Finkbeiner, D.P., & Davis, M. 1998, *ApJ*, 500, 525
- Sguera, V., Hill, A.B., Bird, A.J., et al. 2007, *A&A*, 467, 249
- Skrutskie, M.F., Cutri, R.M., Stiening, R., et al. 2006, *AJ*, 131, 1163
- Sidoli, L., Belloni, T., & Mereghetti, S. 2001, *A&A*, 368, 835
- Stephen, J.B., Bassani, L., Malizia, A., et al. 2006, *A&A*, 445, 869
- Tomsick, J.A., Chaty, S., Rodriguez, J., Walter, R., & Kaaret, P. 2009, *ApJ*, 701, 811
- Torres, M.A.P., Steeghs, D., Jonker, P.G., et al. 2007, *ATel* # 1286
- Tueller, J., Baumgartner, W.H., Markwardt, C.B., et al. 2010, *ApJS*, 186, 378
- Ubertini, P., Lebrun, F., Di Cocco, G., et al. 2003, *A&A*, 411, L131
- van Leeuwen, F. 2007, *A&A*, 474, 653
- Veilleux, S., & Osterbrock, D.E. 1987, *ApJS*, 63, 295
- Vestergaard, M. 2002, *ApJ*, 571, 733
- Vestergaard, M. 2004, *Black-Hole Mass Measurements*, in: *AGN Physics with the Sloan Digital Sky Survey*, ed. G.T. Richards & P.B. Hall, *ASP Conf. Ser.*, 311, 69 (San Francisco: Astronomical Society of the Pacific)
- Voges, W., Aschenbach, B., Boller, T., et al. 1999, *A&A*, 349, 389
- Voges, W., Aschenbach, B., Boller, T., et al. 2000, *IAU Circ.* 7432
- Walter, R., Zurita Heras, J., Bassani, L., et al. 2006, *A&A*, 453, 133
- Warner, B. 1995, *Cataclysmic variable stars* (Cambridge: Cambridge University Press)
- Watson, M.G., Schröder, A.C., Fyfe, D., et al. 2009, *A&A*, 493, 339
- Wegner, W. 1994, *MNRAS*, 270, 229
- Winkler, H. 1992, *MNRAS*, 257, 677
- Winkler, C., Courvoisier, T.J.-L., Di Cocco, G., et al. 2003, *A&A*, 411, L1
- Wright, E.L. 2006, *PASP*, 118, 1711
- Wu, X.-B., Wang, R., Kong, M.Z., Liu, F.K., & Han, J.L. 2004, *A&A*, 424, 793